

Stevens Institute of Technology

FACILITY FORM 602

N 68-28055 (THRU) **1**

(ACCESSION NUMBER)

98 (PAGES) (CODE)

02-95354 (NASA CR OR TMX OR AD NUMBER) (CATEGORY) **10**

Electrical Engineering Department

Program in
Electro-
Physical
Studies

Report EP-1

Microcircuit Models and Diagnostic
Techniques for Environmental Failure
Mode Prediction

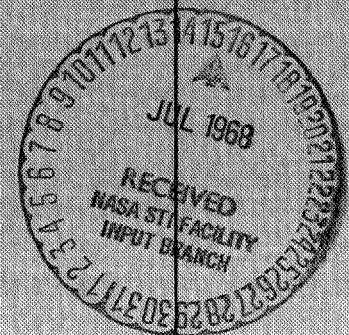
NASA Grant NGR 31-003-050

G. J. Herskowitz

T. J. Kobylarz

E. Zeheb

May 1968



**MICROCIRCUIT MODELS AND DIAGNOSTIC TECHNIQUES
FOR ENVIRONMENTAL FAILURE MODE PREDICTION**

by

**G. J. Herskowitz, Principal Investigator
T. J. Kobylarz
E. Zeheb**

**Prepared For
NASA Electronics Research Center
Under
NASA Research Grant NGR 31-003-050**

**Department of Electrical Engineering
Stevens Institute of Technology
Hoboken, New Jersey**

May, 1968

ACKNOWLEDGEMENT

The authors gratefully acknowledge the programming assistance of Mr. Adolph Vieth of the Electrical Engineering Department and Mr. Raymond Bober of the Stevens Computer Center. The manuscript was edited by Mrs. Lucia Kyriakou, typed by Miss Joan Sudia, and most of the art work prepared by Miss Mary Ann Gentile.

TABLE OF CONTENTS

	<u>Page</u>
1. INTRODUCTION	1
2. MODELING ENVIRONMENTAL EFFECT IN MICROCIRCUITS USING LINVILL LUMPED-PARAMETER ELEMENTS	3
2.1 Relationship Between Linvill Model Elements and Environmental Effects	3
2.2 Linvill Model of a Typical Microcircuit Device	11
3. SENSITIVITY ORIENTED FAILURE MODE DIAGNOSTICS	22
3.1 Failure Mode Prediction	22
3.2 Calculation of Statistical Tolerance Function ΔF_s	23
3.3 Microcircuit Design Based Upon Failure Diagnostics	25
4. A NONLINEAR VERSION OF NASAP	27
4.1 Basic Organization of the Program	27
4.2 Limitations	29
4.3 Determination of the State Equations	32
4.4 Integration	39
5. SUMMARY AND CONCLUSIONS	43
REFERENCES	45

TABLE OF CONTENTS (Con't.)

APPENDICES:

- | | |
|---|-----|
| A. ACTIVE RC FILTER TRANSFER FUNCTION AND SENSITIVITY ANALYSIS USING NASAP | a-1 |
| B. ANALYSIS OF LINEAR INTEGRATED CIRCUITS UNDER THE EFFECTS OF RADIATION USING THE LINVILL MODEL | b-1 |
| C. AUTOMATED DESIGN OF NETWORKS WITHIN SPECIFIED RESPONSE AND IMPEDANCE CONSTRAINTS | c-1 |
| D. MICROCIRCUIT FILTER DESIGN WITH COMPUTER ORIENTED OPTIMIZATION | d-1 |
| E. SENSITIVITY AND WORST CASE COMPUTATIONS FOR NONLINEAR SYSTEMS | e-1 |
| F. APPLICATION OF NONLINEAR NASAP PROGRAM TO THE ANALYSIS OF LINVILL LUMPED-PARAMETER DEVICE MODELS | f-1 |

1. INTRODUCTION

Techniques are described in this report for the prediction of modes of failure when microcircuits are operated under adverse environmental conditions. These failure modes are determined by computer, using systematic modeling and diagnostic techniques which relate microcircuit structure and material properties to the radiation and thermal effects producing them. Design procedures for desensitizing microcircuits to adverse environmental conditions are developed, based upon the analytic techniques for failure mode prediction.

Thermal and radiation effects in semiconductor materials and devices are well documented.¹⁻⁴ Modeling procedures have been proposed for representing thermal, ionizing, and permanent radiation effects in semiconductor devices.^{5,6} These techniques utilize the Ebers and Moll,⁷ charge-control,⁸ or Linvill lumped-parameter⁹ models to determine the effects of environmental conditions on the operation of these devices. The complexity of microcircuit technology suggests the use of a systematic modeling procedure based directly on physical processes and geometries.¹⁰ Modifications of the Linvill lumped-parameter modeling elements have been used in the research described in this report to describe microcircuit behavior under adverse environmental conditions. By using these elements, excellent contact is maintained with physical processes and the effects of radiation and thermal energies upon the microcircuit may be analyzed accurately.

A large number of electronic circuit analysis and design computer

programs are available¹¹ and others are currently under development.¹²

One of these programs, called NASAP (Network And Systems Analysis Program),¹³ is based upon flowgraph techniques.¹⁴ This program has been employed in the analysis of microcircuits^{15,16} and in the evaluation of radiation effects in semiconductor devices.¹⁷ The program has symbolic gain and sensitivity analyses capabilities¹⁸ which enable a determination of the significant micro-circuit structure and material properties which fail. These program features were used as a basis for the microcircuit and diagnostic design techniques described in this report.

One of the major problem areas encountered in the failure mode prediction studies described in this report was that of nonlinear effects occurring because of large environmental disturbances. This required the development of a nonlinear capability for the NASAP program, previously restricted to linear analysis. Algorithms for the nonlinear version of NASAP are described¹⁹ with their application to the analysis of networks with nonlinear Linvill lumped-parameter elements.²⁰

2. MODELING ENVIRONMENTAL EFFECTS IN MICROCIRCUITS USING LINVILL LUMPED-PARAMETER ELEMENTS

In the Linvill lumped-parameter approach to modeling semiconductor devices, excellent contact is maintained with physical processes. Radiation and thermal effects are traceable directly to the material properties. The Linvill model, therefore, provides an exact means of obtaining a physical picture of device behavior under adverse environmental conditions. The effects of radiation and thermal energies on each of the parameters which are used to describe device behavior with the Linvill model will be examined. The Linvill model for a particular microcircuit device will then be developed from its structure and material properties.

2.1 Relationship Between Linvill Model Elements and Environmental Effects

The essence of the Linvill lumped-parameter approach to modeling semiconductor devices is the removal of space variables from the partial differential equations describing current continuity, and lumping regions of the material by the method of finite differences.⁹ A number of points are selected within the semiconductor material; their selection depends on the rapidity of change in the properties of the material in the region under consideration. Then, the continuity equations at each of the points are approximated by writing the spatial derivatives in terms of differences between densities at adjacent points. Time derivatives are maintained in differential form. As an example of the procedure, consider the cube of semiconductor material shown in Fig. 1. The continuities of electron and hole charge densities in this region is given by the equations

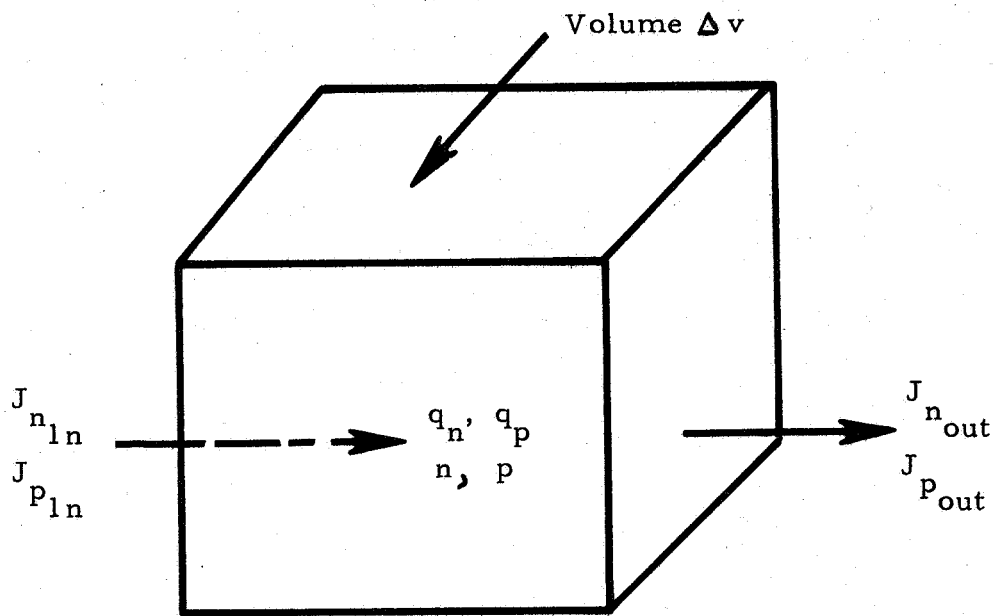


FIG. 1 CUBE OF SEMICONDUCTOR MATERIAL REPRESENTING LUMP OF LINVILL MODEL

$$\frac{\partial q_n}{\partial t} = \nabla \cdot \bar{J}_n - \frac{1}{\tau_n} (q_n - q_{no}) + g_n \quad (1)$$

$$\frac{\partial q_p}{\partial t} = \nabla \cdot \bar{J}_p - \frac{1}{\tau_p} (q_p - q_{po}) + g_p \quad (2)$$

where

q_n, q_p are the electron and hole carrier charge densities (coul/cm³)

q_{no}, q_{po} are the electron and hole equilibrium charge densities (coul/cm³)

\bar{J}_n, \bar{J}_p are the electron and hole current densities (ampere/cm²)

τ_n, τ_p are the effective lifetimes of electrons and holes (seconds)

g_n, g_p are the rates at which electron and hole charges are generated (coul/cm³ - sec)

Equations (1) and (2) describe how the electron and hole carrier charge densities, q_n and q_p , change with time due to:

1. Storage of charge in the lump.
2. Recombination of charge.
3. Generation of charge.

Each of these effects is represented by a network-like element in the Linvill model. First, consider the total charge stored in the lump,

$$Q_n + Q_p = \oint_{\text{volume}} q_n dv + \oint_{\text{volume}} q_p dv = S_n n + S_p p \quad (3)$$

where Q_n and Q_p are the total electron and hole carrier charges stored in the lump and S_n, S_p are the Linvill elements called electron and hole "storances" given by $S = q \Delta v$. Note that the storance is defined in terms of q , the charge of an electron (1.6×10^{-19} coul), and Δv , the incremental lump volume, and is therefore a function of geometry only. The electron and hole carrier

densities, n and p , have been factored out of Q_n and Q_p as the charge density variables. This allows the circuit analyst to proceed directly from device geometry when using the Linvill model. The current component due to displacement of charge in the lump is given by

$$i_{\text{displ}} = \frac{dQ_n}{dt} + \frac{dQ_p}{dt} = S_n \frac{dn}{dt} + S_p \frac{dp}{dt} \quad (4)$$

Carrier charge recombination is represented by the second terms on the right sides of Equations (1) and (2). Each of these terms may be thought of as a current density generator proportional to the excess electron densities, $q_n - q_{no}$ and $q_p - q_{po}$, and inversely proportional to the effective carrier lifetimes τ_n and τ_p .

The temperature dependence of effective carrier lifetimes τ_n and τ_p may be obtained from the Shockley-Read Theory.²¹ According to this theory, the effective lifetime of carriers in a semiconductor material with both free electron and hole carriers is given by

$$\tau = \frac{n_i^2}{q(p+n)} \quad (5)$$

where

$$n_i^2 = 15 \times 10^{32} T^3 e^{-1.21/kT}$$

T = Temperature ($^{\circ}\text{K}$)

k = Boltzman's Constant (1.38×10^{-23} Joules/ $^{\circ}\text{K}$).

The temperature dependence of τ_n and τ_p for a particular N or P type material may be found by using the approximations $n \gg p$ or $p \gg n$. The current components resulting from recombination of charge in the lump are given by

$$i_{nr} = \frac{1}{\tau_n} (Q_n - Q_{no}) = H_{cn} (n - n_0)$$

$$i_{pr} = \frac{1}{\tau_p} (Q_p - Q_{po}) = H_{cp} (p - p_0)$$
(6)

where $H_c = q \Delta v / \tau$ is termed the "combinance". It is a function of both the geometry and effective carrier lifetime in the material. Note that one carrier (either n or p) predominates in the material and recombination is ignored for that carrier in the model.

When considering radiation effects in semiconductors, the effective carrier lifetime is a key property of the material, since τ is related to the radiation damage in semiconductor materials by the fundamental equation³

$$\frac{1}{\tau_\phi} = \frac{1}{\tau_0} + \frac{\Phi}{K}$$
(7)

where τ_ϕ is the effective lifetime at some exposure, τ_0 is the initial lifetime, and K is the damage constant dependent on material, doping, and energy spectrum of the incident particle fluence, Φ . Note that the ratio

$$\frac{H_c}{S} = \frac{1}{\tau_\phi}$$
(8)

produces this relationship directly, and therefore will be an important parameter in analyzing semiconductor devices and integrated circuits for radiation damage effects when using the Linvill model.

Carriers may be generated by incident radiation at a rate g which is dependent on the rate of energy absorption through the ionization of neutral atoms to form free charge carriers according to the expression³

$$g = k_g \dot{\gamma}$$
(9)

where k_g is the energy-dependent generation constant for a particular material

and γ is the exposure rate (R/sec).

Linville did not consider the

generation of carriers above an equilibrium value in his original model.

However, a current generator related to storance may be included in the model

to account for charge carrier generation,

$$i_g = q \Delta v g = S k_g \dot{\gamma} \quad (10)$$

Note that, unlike the elements defined for charge storage and recombination,

the generation current generator is independent of the charge density variables.

In addition to the effects described above for a single lump of semiconductor material, current flows between lumps due to diffusion and drift of

charge. The equations which describe the flow of current between lumps

i and j of a semiconductor material separated by an average distance Δx_{ij} are:

$$J_n = q_n \mu_n E + D_n \frac{q_{n_i} - q_{n_j}}{\Delta x_{ij}} \quad (11)$$

$$J_p = q_p \mu_p E - D_p \frac{q_{p_i} - q_{p_j}}{\Delta x_{ij}} \quad (12)$$

where

μ_n and μ_p are the electron and hole mobilities ($\text{cm}^2/\text{volt-sec}$)

E is the electric field (volts/sec)

D_n and D_p are the electron and hole diffusion constants ($\text{cm}^2/\text{volt-sec}$)

Thermal energy effects the transport properties of semiconductor materials through the electron and hole mobilities μ_n and μ_p and diffusion constants D_n and D_p .¹ The magnitude of mobility depends on the nature and density of scattering centers present and on the average thermal velocity

of the carriers. Scattering centers are caused primarily by thermal vibrations of the lattice and impurity ions according to the relationship

$$\frac{1}{\mu} = \frac{1}{\mu_L} + \frac{1}{\mu_I} \quad (13)$$

where

μ_L = lattice mobility

μ_I = impurity mobility

Theoretical expressions for the lattice mobility μ_L have been derived,²² but for actual calculations the following empirical values are usually employed for silicon¹:

$$\begin{aligned} \mu_{nL} &= 2.1 \times 10^9 \times T^{-2.5} \text{ cm}^2 \text{ v}^{-1} \text{ sec}^{-1} \\ \mu_{pL} &= 2.3 \times 10^9 \times T^{-2.7} \text{ cm}^2 \text{ v}^{-1} \text{ sec}^{-1} \end{aligned} \quad (14)$$

T is temperature in degrees Kelvin.

Calculations of impurity mobility μ_I ²³ indicate that this component of mobility is inversely proportional to the density of impurity ions (ionized donor and acceptor atoms) and increases with temperature T at a rate proportional to $T^{3/2}$. The connection between diffusion constant D and total mobility μ is shown through statistical arguments to be the Einstein relationship¹

$$D = (kT/q) \mu \quad (15)$$

The diffusion current between lumps depends on the charge difference ΔQ_{ij} and may be written, for one-dimensional current flow, as

$$i_{\text{diff}} = D \frac{\Delta Q_{ij}}{\Delta x_{ij}} = H_d (n_i - n_j) \quad (16)$$

where $H_d = q \frac{AD}{\Delta x_{ij}}$ and is termed "diffusance" (A is the average area of the lump). A similar hole current flows between lumps when the hole carrier charges are significantly different between lumps. However, for most semiconductor materials, one carrier predominates (majority carrier), and charge differences produce small gradients, and therefore the diffusion term may be neglected for these carriers unless there is a very large difference in carrier densities between lumps.

The drift component of current between lumps may be written in terms of the "driftance" F_d as

$$i_{\text{drift}} = Q\mu E = F_d \frac{(n_i + n_j)}{2} \quad (17)$$

where $F_d = \frac{(v_i - v_j)}{\Delta x_{ij}} qA\mu$. The factor $(v_i - v_j)$ is the voltage difference between lumps i and j. This voltage difference is generally quite small and the drift component may be neglected, except in the following cases:

1. Voltage difference is fixed by the diffusion profile (for example, a drift transistor).
2. High current densities (possibly produced by large radiation fields) cause an ohmic drop in the bulk material.

In the first case, the drift term is linear since the field producing the drift component of current is constant. However, in the second case, the field is dependent upon the current density, which in turn produces the drift current, thus resulting in a nonlinear situation. A nonlinearity of this type may be handled by using nonlinear network techniques described in a later section of this report.

The symbols used to describe the Linvill elements with radiation and thermal effects and the equations describing each element are summarized in Table I. A typical interconnection of the elements of two adjacent lumps of semiconductor material is shown in Fig. 2.

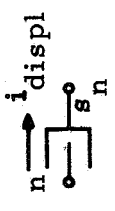

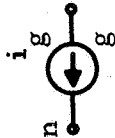
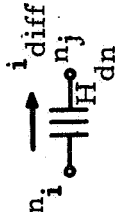
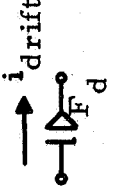
2.2 Linvill Model of a Typical Microcircuit Device

The elements developed in the last section for modeling semiconductor devices and microcircuits when under the influence of radiation and thermal effects will be employed to model a typical structure. First, however, the semiconductor junction must be described and modeled. PN junctions are diffused into semiconductor material to form the devices and circuits. They manifest themselves two ways: they impose boundary conditions upon the charge densities at the edges of the bulk material and, second, the space charge within the depletion region results in a "depletion capacitance" associated with the junction. Assuming that there is no recombination within the depletion region and that continuity of hole and electron currents is maintained across the depletion region, the carrier densities just outside the depletion region of the junction are given by "the law of the junction";

$$\begin{aligned} p &= p_n \exp. qV/kT && \text{for N-type material and} \\ n &= n_p \exp. qV/kT && \text{for P-type material} \end{aligned} \tag{18}$$

where V is the voltage applied across the depletion region and p_n and n_p are the boundary values of holes and electrons at the junction. The junction capacitance is determined from the charge distribution in the depletion region. The general expression for this capacitance is

TABLE I SUMMARY OF LINVILL ELEMENTS

ELEMENT	DEFINITION	SYMBOL	TERMINAL CURRENT
STORAGE	$S = q \Delta V$		$i_{\text{displ}} = S \frac{dn}{dt}$
COMBINANCE	$H_c = q \Delta V \left(\frac{1}{\tau_0} + K\Phi \right)$		$i_r = H_{cn} (n - n_0)$
CARRIER GENERATION	$g = k\dot{\gamma}$		$i_g = Sk\dot{\gamma}$
DIFFUSANCE	$H_d = \frac{qAD}{\Delta x_{ij}}$		$i_{\text{diff}} = H_{dn} (n_i - n_j)$
DRIFTANCE	$F_d = \frac{(v_i - v_j)}{\Delta x_{ij}} q A\mu$		$i_{\text{drift}} = F_{dn} \left(\frac{n_i + n_j}{2} \right)$

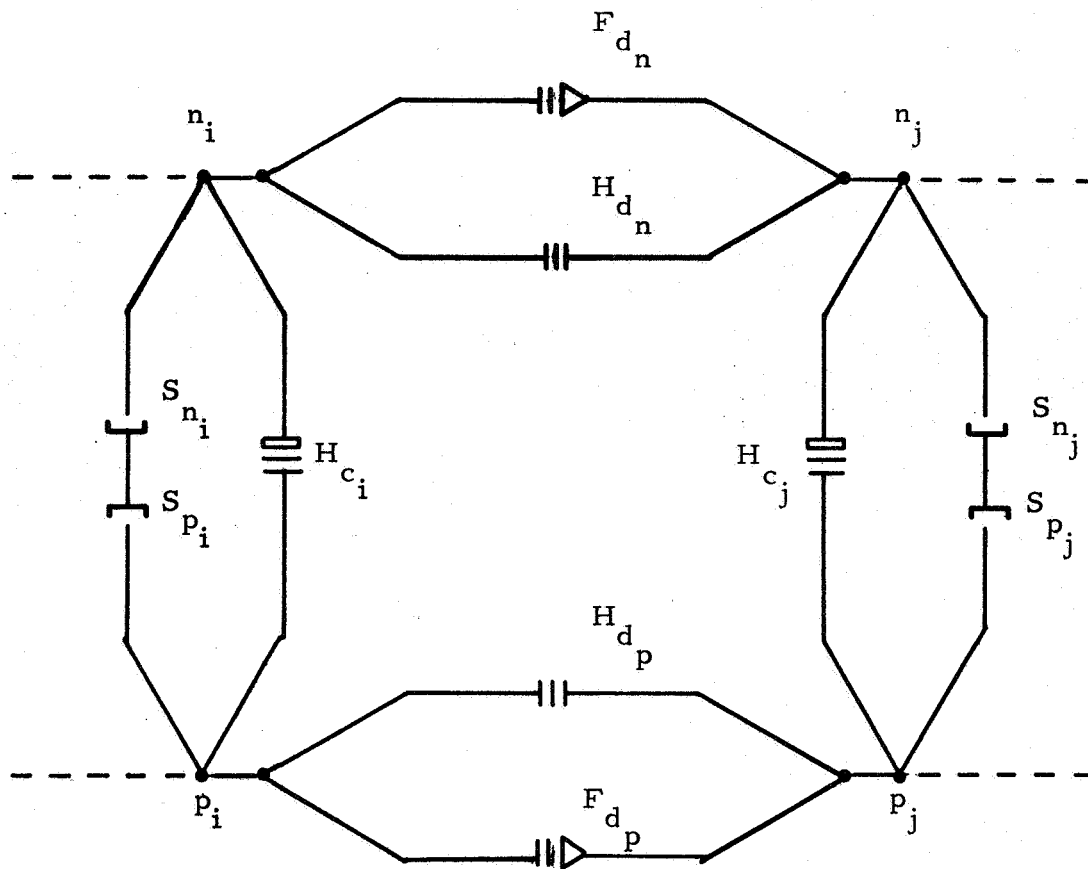


FIG. 2 TYPICAL INTERCONNECTION OF LINVILL ELEMENTS FOR TWO ADJACENT LUMPS

$$C_d = \frac{Q_d}{V} \quad (19)$$

where Q_d is the total charge in the junction depletion region and V is the voltage across this region. The capacitance calculation is based upon the impurity profile of the junction diffusion.

A typical transistor may be represented by the Linvill model of Fig. 3 for low carrier densities and space-charge neutrality when the drift component of current is neglected and $S_n \frac{dn}{dt} = S_p \frac{dp}{dt}$. The model may be described by the following parameters: S_1 , H_{c1} , H_d , H_{c2} , S_2 , C_{BE} , and C_{BC} . In order to demonstrate the relationship of these parameters to geometry in an idealized example, an integrated circuit transistor configuration,²⁴ shown in Fig. 4, will be used. The primary interaction to be considered of the integrated circuit transistor with the remaining part of the circuit is the collector-substrate capacitance C_{cs} . In general, many other interactions exist.¹⁰

The first step in the procedure of modeling the integrated circuit transistor of Fig. 4 is to examine the emitter-base, base-collector and collector-substrate depletion regions. This is accomplished with the aid of the approximate doping profile given in Fig. 4 beside the geometrical configuration. The actual profile for this structure consists of a combination of complementary error functions and Gaussian distributions.²⁴ However, for the purpose of simplifying the example given here, the approximate distribution of Fig. 4 will be used.

Based on the simplified model, the step-junction capacitance is given by

$$C = \frac{A(\epsilon N_a N_d)^{1/2}}{(V_{BE} - V_b)^{1/2} [2(N_a + N_d)]^{1/2}} \quad (20)$$

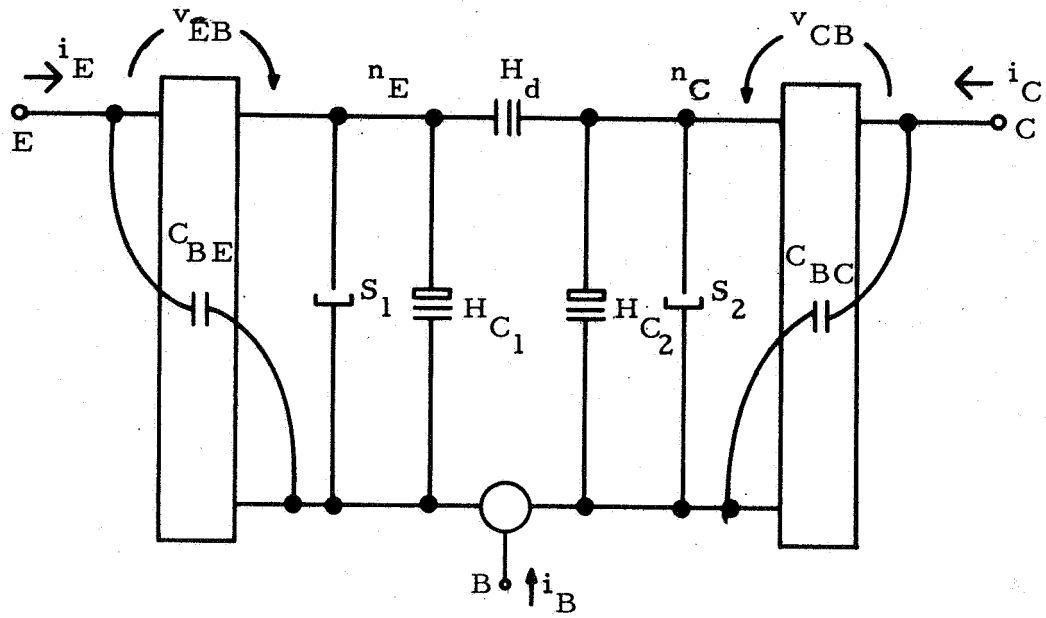


FIG.3 TWO LUMP LINVILL MODEL OF DIFFUSION TRANSISTOR

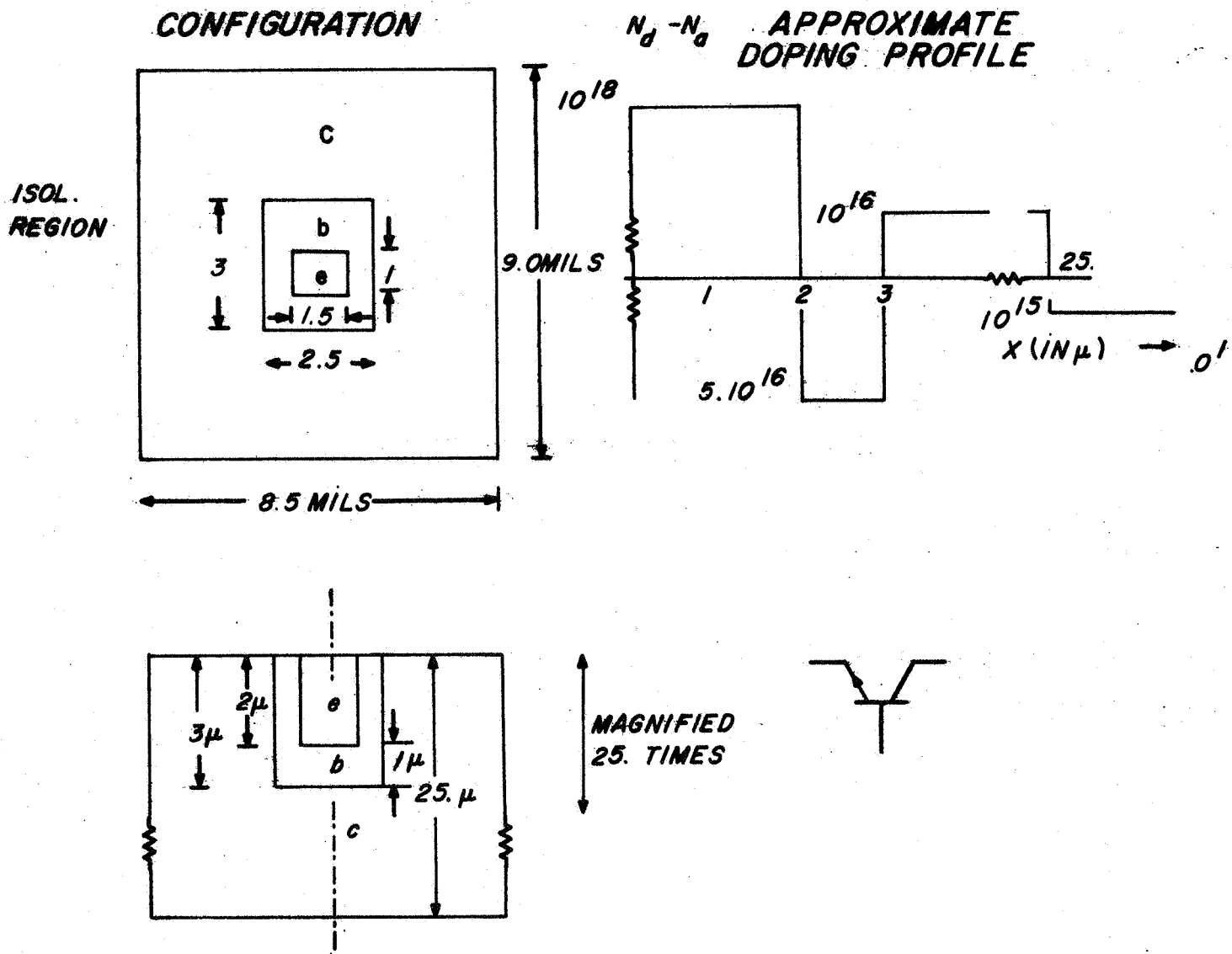


FIG. 4 INTEGRATED CIRCUIT TRANSISTOR CONFIGURATION

where V_b is the barrier voltage, given by

$$V_b = \frac{-kT}{q} \ln \frac{N_a N_d}{N_b^2}$$

N_a = Number of ionized acceptor atoms in emitter and collector regions (10^{16} and 10^{18} atoms/cm³ respectively)

N_d = Number of ionized donor atoms in the base region (5×10^{16} atoms/cm³)

and ϵ is the permittivity of the material ($12\epsilon_0$ for silicon).²⁵ The resulting capacitances at zero bias are

$$C_{BE}(0V) = 0.71 \text{ pf}$$

$$C_{BC}(0V) = 1.48 \text{ pf}$$

A negative bias of 5 volts will reduce C_{BC} to 0.53 pf. Assuming that the collector-substrate junction is reverse biased at -5 volts for isolation,

$$C_{CS} = 1.81 \text{ pf.}$$

The next step in determining the transistor model is to evaluate the elements in the two-lump model of the base region of Fig. 3. This is accomplished by examining the base parallelepiped of Fig. 5a. The resulting calculations proceed as follows:

1. Divide the base region in two lumps, each having a volume

$$\Delta V = \frac{A \ell}{2} = \frac{(9.68 \times 10^{-4}) (10^{-4})}{2} = 4.84 \times 10^{-10} \text{ cm}^3.$$

2. $S_1 = S_2 = q \Delta V = (1.6 \times 10^{-19}) (4.84 \times 10^{-10}) = 7.75 \times 10^{-29} \text{ coul cm}^3.$

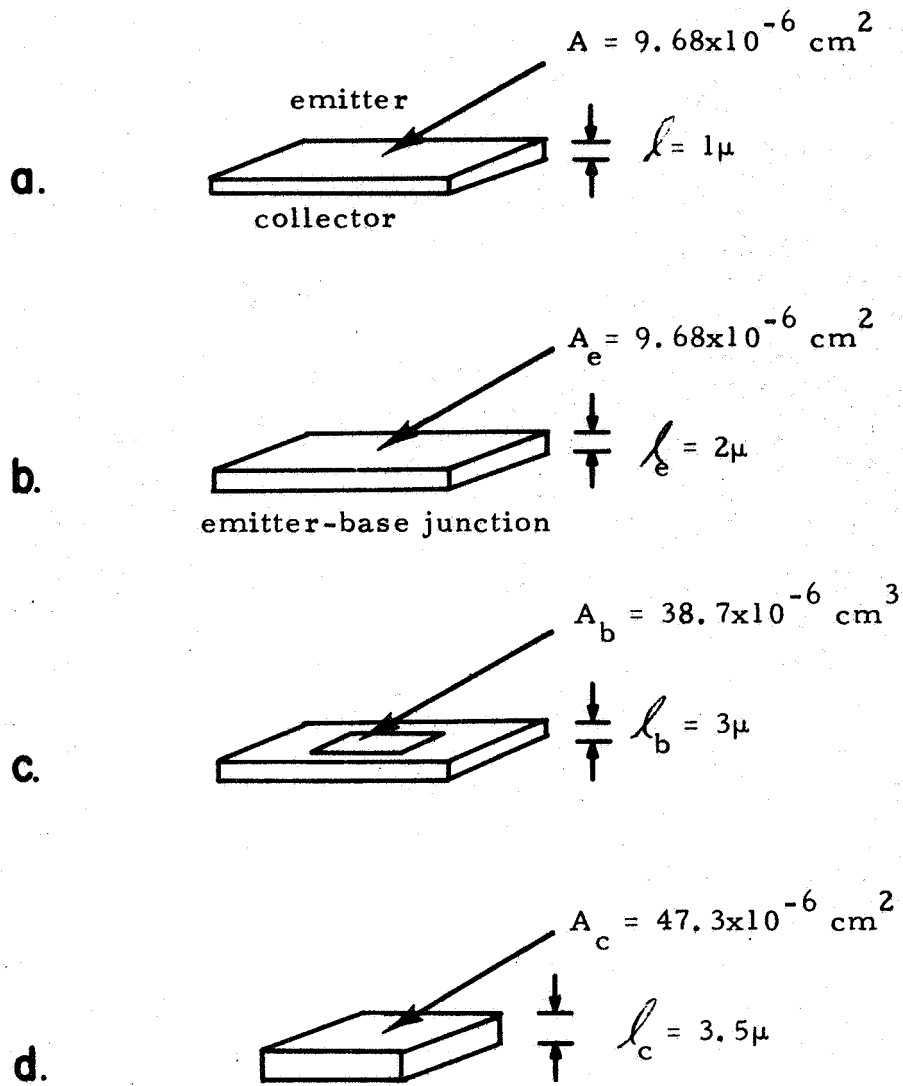


FIG. 5 REGIONS OF CONSIDERATION IN MODEL

$$3. H_{c1} = \frac{S}{\tau_{ne}} = \frac{7.75 \times 10^{-29}}{\tau_{ne}} \text{ amp cm}^3.$$

$$4. H_{c2} = \frac{S_2}{\tau_{nc}} = \frac{7.75 \times 10^{-29}}{\tau_{nc}} \text{ coul cm}^3$$

$$5. H_d = \frac{AD_{nq}}{\ell} = \frac{(9.68 \times 10^{-6}) (35) (1.6 \times 10^{-19})}{10^{-4}}$$

$$H_d = 5.42 \times 10^{-19} \text{ Amp cm}^3$$

Note that H_{c1} and H_{c2} are left in terms of their respective lifetimes, τ_{ne} and τ_{nc} . This allows us to use these parameters later with Eq. 6 to determine the effect of radiation damage on a device of this type operating in a linear or digital circuit.

Additional elements could be added to the basic model of Fig. 3 to account for the emitter body, Fig. 5b, base bordering the emitter, Fig. 5c, and the collector body below the active region, Fig. 5d. A complex model, including all of these effects and the collector-substrate capacitance is shown in Fig. 6. The additional elements, calculated in an analogous manner to the above, are:

$$S_e = 3.10 \times 10^{-28} \text{ coul cm}^3$$

$$H_{ce} = \frac{3.10 \times 10^{-28}}{\tau_{pe}} \text{ amp cm}^3$$

$$S_b = 1.86 \times 10^{-27} \text{ coul cm}^3$$

$$H_{cb} = \frac{1.86 \times 10^{-27}}{\tau_{cb}} \text{ amp cm}^3$$

$$S_c = 2.66 \times 10^{-23} \text{ coul cm}^3$$

$$H_{cc} = \frac{2.66 \times 10^{-23}}{\tau_{pc}} \text{ amp cm}^3$$

The number of elements in the model used in the analysis of a particular circuit depends upon the accuracy desired in the computer solution. The operation of a typical linear integrated circuit in a radiation environment has been analyzed with the aid of the NASAP computer program. The equivalent circuit coding for NASAP is presented together with the results of the analysis in Appendix B.

3. SENSITIVITY ORIENTED FAILURE MODE DIAGNOSTICS

Failure mode prediction may be achieved using first derivative information of microcircuit element variations when changes are considered incremental. In the case of environmental conditions, the microcircuit model elements described in Section 2 are continuous functions of radiation and temperature. Therefore, a sensitivity approach, based on first derivative information of element variation, will be employed to determine modes of microcircuit failure.

3.1 Failure Mode Prediction

The criterion used to determine when a microcircuit operating in adverse environments has failed determines how the prediction analysis is formulated. There are several methods of calculating a change in network variable F for a change in elements e_k having nominal values e_k^o .²⁶ If the network function F is a function of the elements e_k (for small changes, Δe_k in N elements), the change in F is

$$\Delta F = \sum_{k=1}^N \Delta e_k \left. \frac{\partial F}{\partial e_k} \right|_{e_k = e_k^o} \quad (21)$$

This derivative information may be used in one of three ways:

1. If the Δe_k are known precisely, ΔF may be estimated from Eq. (21).
2. If the Δe_k are assumed to lie within the tolerance limits ϵ_k , i. e., $-\epsilon_k \leq \Delta e_k \leq \epsilon_k$, the largest possible variation in F may be estimated as

$$\Delta F_{\max} = \sum_{k=1}^N (\pm \epsilon_k) \frac{\partial F}{\partial e_k} \quad (22)$$

where the sign of ϵ_k is chosen the same as that of the derivative; ΔF_{\max} represents the worst-case.

3. If the Δe_k are described by probability distributions, then a distribution for ΔF may be estimated by statistical methods. The statistical tolerance ΔF_s is defined as

$$\Delta F_s = \left[\left(\frac{\partial F}{\partial e_1} de_1 \right)^2 + \dots + \left(\frac{\partial F}{\partial e_k} de_k \right)^2 + \dots + \left(\frac{\partial F}{\partial e_N} de_N \right)^2 \right]^{1/2} \quad (23)$$

where ΔF_s is a measure of the deviation of F from its mean value due to deviations of the elements from their respective mean values.

In formulating a meaningful failure mode prediction criterion, it is necessary to decide which of the above formulations is appropriate. Since the interactions of environmental effects on microcircuits are known only on a statistical basis, the statistical tolerance T_F , defined by Eq. (23), appears to be the most meaningful criterion for failure mode prediction from first derivative information. If T_F is a threshold above which the deviated network function $\left| F \pm \Delta F_s \right|$ fails to meet its specified requirements, then the failure mode criterion is given by

$$\left| F \pm \Delta F_s \right| > T_F \quad (24)$$

3.2 Calculation of Statistical Tolerance Function ΔF_s

The statistical tolerance function ΔF_s may be expressed in terms of a relative sensitivity of F with respect to a relative change in e_k ;

$$\Delta F_s = \left[\sum_{k=1}^N \left| S_{e_k}^F \frac{de_k}{e_k} \right|^2 \right]^{1/2} F \quad (25)$$

where $S_{e_k}^F$ is the percent change in F due to a percent change in e_k , expressed as

$$S_{e_k}^F = \frac{\partial \ln F}{\partial \ln e_k} = \frac{e_k}{F} \frac{\partial F}{\partial e_k} \quad (26)$$

Computer methods of calculating ΔF_s , using the form of Eq. (25), are based upon the NASAP program. This computer program is ideal for calculating the network function F ¹³ and sensitivity functions $S_{e_k}^F$.¹⁸ It is based upon writing the network equations in flowgraph form.¹⁴ An example of the use of this program in computing the network transfer function and sensitivity of an active RC filter has been described.²⁷ This analysis is presented in Appendix A.

Once the network function F and sensitivity functions $S_{e_k}^F$ are determined using the NASAP program, the relative changes in element values $\frac{de_k}{e_k}$ due to environmental conditions must be determined. For radiation Φ and temperature T effects, these variations are computed using the expression

$$\frac{de_k}{e_k} = \frac{1}{e_k} \left[\frac{\partial e_k}{\partial \Phi} d\Phi + \frac{\partial e_k}{\partial T} dT \right] \quad (27)$$

where e_k are the nominal element values, and $d\Phi$ and dT are the increments in radiation level and temperature causing element variations $\frac{\partial e_k}{\partial \Phi}$ and $\frac{\partial e_k}{\partial T}$.

For the Linvill lumped-parameter elements described in Section 2, the variation in "combinance" H_c , "diffusance" H_d and "driftance" F_d may be found by examining the radiation and temperature effects on effective carrier lifetime τ ,

mobility μ , and diffusance D given in Eqs. (5), (7), (14) and (15). These first order partial derivatives are listed in Table II for variations due to radiation Φ and temperature T .

3.3 Microcircuit Design Based Upon Failure Diagnostics

The statistical tolerance function ΔF_s , described for use in failure mode diagnostics in Section 3.1, may also be used advantageously in designing microcircuits which are desensitized to environmental conditions. If it is desired to maintain a network function F below a certain threshold level T_F to prevent the response from exceeding allowable bounds of acceptable behavior, the statistical tolerance function ΔF_s , as calculated from the NASAP program in Section 3.2, may be used to achieve this design objective. One such procedure,³¹ based upon continuously equivalent network theory,³² is outlined in Appendix C. Another procedure, based upon the work of E. Zeheb, is given in Appendix D. Each of these methods has still to be fully implemented and exemplified. It is expected that the subject of the next Progress Report will be devoted to a description of the application of these two methods to automated communication circuit design with NASAP.

TABLE II

Lumped-Element First Order Partial Derivatives
For Failure Mode Analysis

$$\frac{\partial H_c}{\partial \Phi} = \frac{q \Delta v}{K}$$

$$\frac{\partial H_c}{dT} = \frac{q^2 \Delta v (n+p)}{15 \times 10^{32}} \left[\frac{1.21}{(kT)^2} T^{-3} \epsilon^{\frac{1.21}{kT}} - 3T^{-4} \epsilon^{\frac{1.21}{kT}} \right]$$

$$\frac{\partial F_d}{d\Phi} = 0$$

$$\frac{dF_d}{dT} = \frac{(v_i - v_j)}{\Delta x_{ij}} qA \left[\frac{\frac{d\mu_L}{dT} / \mu_L^2 + \frac{d\mu_I}{dT} / \mu_I^2}{\left(\frac{1}{\mu_L} + \frac{1}{\mu_I} \right)^2} \right]$$

where

$$\frac{d\mu_I}{dT} = \frac{3/2 T^{1/2}}{N_I}$$

$$\frac{d\mu_{nL}}{dT} = -5.25 \times 10^9 T^{-15}$$

$$\frac{d\mu_{pL}}{dT} = -6.21 \times 10^9 T^{-1.7}$$

For Silicon

$$\frac{\partial H_d}{\partial \Phi} = 0$$

$$\frac{\partial H_d}{\partial T} = \frac{kTA}{\Delta x_{ij}} \left[\frac{\frac{d\mu_L}{dT} / \mu_L^2 + \frac{d\mu_I}{dT} / \mu_I^2}{\left(\frac{1}{\mu_L} + \frac{1}{\mu_I} \right)^2} \right]$$

4. A NONLINEAR VERSION OF NASAP

This section presents an overview of a nonlinear network analysis program which is based on the fundamental principles of the linear network analysis program NASAP.⁴¹⁻⁴³ A number of details, omitted in this report, can be found in a preceding progress report.¹⁹ Several developments subsequent to the progress report are discussed here and in the appendix. These include the availability of nonlinear dependent sources for circuits, algorithms for sensitivity and worst-case analysis of nonlinear networks, and the application of the program to nonlinear Linvill lumped-parameter models of semiconductor devices.

4.1 Basic Organization of the Program

The program will accept circuits consisting of 9 different types of elements. The elements are described in Table III. All of the elements can be linear or nonlinear functions of the arguments. Any function which can be written in FORTRAN is applicable for describing the element behavior. In addition, the functions can be described by a table of values. Linear interpolation and extrapolation (piecewise linear) is performed unless otherwise specified. If a function is to be nonlinear between successive points, then a FORTRAN function can be specified by the user.

Linear elements, other than the two generators, can be specified by appropriate constants. For example, one can write $G = 1. / (1. E-6)$ for a $1M\Omega$ resistor.

The program consists of two parts. The input to the first part is a topological description of the circuit. The elements are described by symbols.

TABLE III

Elements Accepted by Program

ELEMENT	RELATIONSHIPS
PASSIVE:	
RESISTOR (resistance form)	$v = Ri$ $v = f_R(i)$
(conductance form)	$i = Gv$ $i = f_G(v)$
CAPACITOR (elastance form)	$v = Sq$ $v = f_S(q)$
INDUCTOR (inverse form)	$i = \Gamma\lambda$ $i = f_\Gamma(\lambda)$
ACTIVE:	
VOLTAGE GENERATOR	$v = f_v(t)$
CURRENT GENERATOR	$i = f_i(t)$
CURRENT AMPLIFIER	$i_2 = \beta i_1$ $i_2 = f_\beta(i_1)$
VOLTAGE AMPLIFIER	$v_2 = \mu v_1$ $v_2 = f_\mu(v_1)$
TRANSCONDUCTANCE	$i_2 = gv_1$ $i_2 = f_g(v_1)$
TRANSRESISTANCE	$v_2 = ri_1$ $v_2 = f_r(i_1)$

UNITS:

v (volts), i (amps), R (ohms), G (mhos), S (darafs)

Γ (henries⁻¹), g (mhos), r (ohms), t (sec.)

The symbols represent constants, if the element is linear, or functions, if the element is nonlinear. The symbols are operated upon to form the circuit state equations. This is in keeping with the NASAP principle of symbol manipulation to allow for network equations as well as numerical results. It is important to point out that FORTRAN is designed for numerical computation and not string manipulation. For this reason a list processing language such as SNOBOL is required for implementation of the algorithms.

The output of the first part will be the network equations written in FORTRAN. This output can be on punched cards so as to alleviate some user labor.

The second part of the program employs the element values and functions as the input. The prototype will compute, in FORTRAN, the transient response of user selected outputs. A graphical output will be provided. It is planned to include sensitivity, worst-case, steady state analysis, determination of stable points, etc., in later versions.

It is, of course, cumbersome for the user to have two separate parts to a program. List processing and numerical computation are available in PL/I. It will be possible to combine the two parts in this language. For this reason, it is suggested that the program be translated into PL/I when the compiler becomes available.

4.2 Limitations

In order to keep the algorithms relatively simple, it was decided to place several restrictions on circuit topology. The basis of the restrictions receives detailed treatment in the aforementioned report.¹⁹ The first restriction is that no loops may exist which consist solely of capacitors, dependent voltage sources

(e. g., transresistance), and independent voltage sources. These elements are viewed as tree branches by the program. Another restriction is that no cut-set may exist which consists of inductors, dependent current sources (e. g., current amplifier), and independent current sources. These elements are viewed as links by the program.

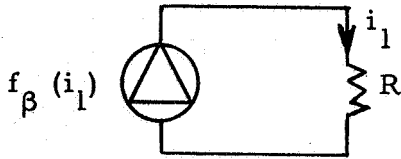
The following two limitations ensure unique solutions as well as simplify the algorithms. Nonlinear resistors of the resistance form (or conductance form) must be in a cut-set (or loop) where the other elements are inductors and current generators (or capacitors and voltage generators). The consequence of this limitation is that the arguments of the resistor nonlinear functions are summations of generator and inductor currents (or generator and capacitor voltages). This ensures a unique determination of resistor voltage (or current).

The second limitation for a unique solution applies to the dependent sources $i_2 = f_\beta(i_1)$ through $v_2 = f_r(i_1)$. The arguments of these functions must be determined by either of the following two conditions:

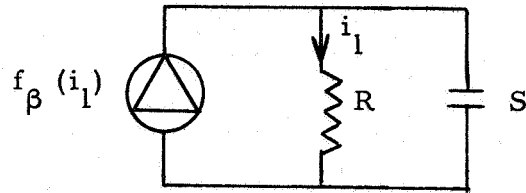
(1) A summation of inductor and generator currents, for a current argument (or a summation of capacitor and generator voltages for a voltage argument).

(2) A current or a voltage of a resistor which is in a loop consisting of capacitors and voltage generators (or a resistor which is in a cut-set consisting of inductors and current generators). The resistor for this condition may be linear or nonlinear .

Figures 7 and 8 are intended to clarify these conditions. In Fig. 7(a),



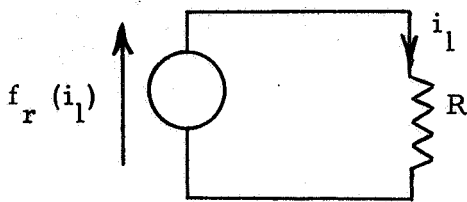
(a) No Unique Solution



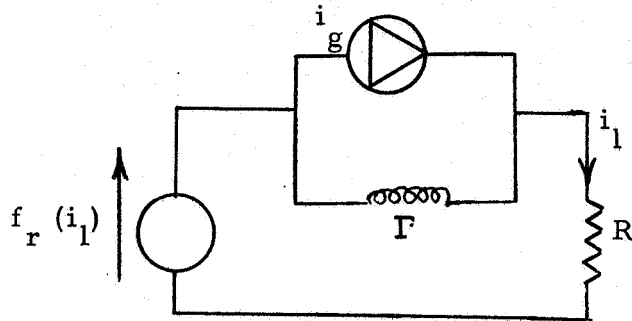
(b) Unique Solution

Fig. 7 CONDITIONS ON

$$f_{\beta}(i_1) = \tan(i_1)$$



(a) No Unique Solution



(b) Unique Solution

Fig. 8 CONDITIONS ON

$$f_r(i_1) = \tan(i_1)$$

infinitely many solutions exist. The circuit in figure 7(b) has a unique solution because the resistor is shunted by a capacitor. The state of the circuit fixes the capacitor voltage. This voltage permits the computation of i_1 , which in turn allows the computation of $f_{\beta}(i_1)$.

Similarly, Fig. 8(a) has no unique solution. The circuit in Fig. 8(b) has a unique solution since i_1 is the sum of the generator current i_g and the inductor current. In this case the total state (input state and internal state) determines i_1 uniquely.

The two preceding conditions are mandatory for the first part of the program if the dependent source is nonlinear. The reason for this is that no provision is made for the inversion of nonlinear functions. Linear dependent

sources which do not satisfy the conditions will be accepted by the first part if the argument is a linear function of the total state. However, the second part may reject the circuit whenever numerical computations are impossible. Figure 9 shows an example of this. The following linear function

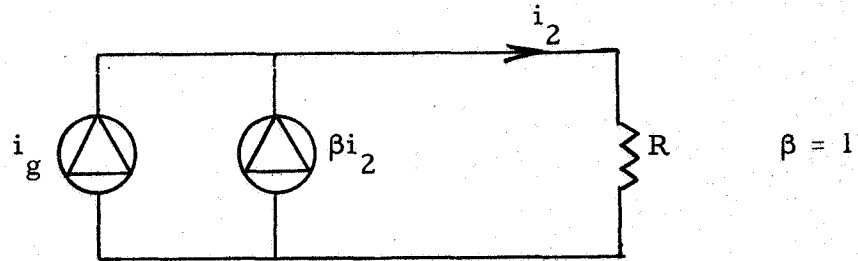


Fig. 9 CIRCUIT REJECTED BY PART 2

will be found in part 1:

$$i_2 = i_g / (1 - \beta)$$

Part 2 will not operate since $\beta = 1$.

In view of the complex topology requirements, diagnostics will be indicated whenever a circuit is rejected. The diagnostics will also suggest parasitic elements which would make the circuit acceptable.

4.3 Determination of the State Equations

The aforementioned progress report showed that equations of the following two forms are tantamount to the system state equations:

$$\underline{v}_L = \underline{G}_L (\underline{v}_c, \underline{i}_L, \underline{i}_g, \underline{v}_g) \quad (28)$$

$$\underline{i}_c = \underline{G}_c (\underline{v}_c, \underline{i}_L, \underline{i}_g, \underline{v}_g) \quad (29)$$

where

\underline{i}_L represents the inductor currents

\underline{v}_L represents the inductor voltages

\underline{i}_c represents the capacitor currents

\underline{v}_c represents the capacitor voltages

\underline{i}_g represents the independent current sources

\underline{v}_g represents the independent voltage sources.

It was further explained that these equations can be obtained from the dichotomous signal-flowgraph by the closed loop concept. The dichotomous signal-flowgraph and the closed loop concept are two further NASAP principles preserved in the nonlinear analysis program.

The program begins by determining a "master" signal-flowgraph from the circuit topology. This is stored as V, W, and T vectors in the computer. The argument ($\underline{v}_c, \underline{i}_L, \underline{i}_g, \underline{v}_g$) of equations (28) and (29) is viewed as a set of sources in the system. The remaining elements are instantaneous in i and v. Hence, an algebraic d-c analysis is performed by part 1 of the program.

A pseudo-superposition procedure which treats one source at a time is used. This corresponds to an iterative application of the closed-loop concept for every source/output combination. The set of outputs consists of $\underline{v}_L, \underline{i}_c$, and any others specified by the user. (Note - Part 2 will only print the results of the user specified outputs.)

After all source/output combinations are exhausted, a factorization procedure is employed to form the nonlinear function arguments. The resulting equations are yielded in FORTRAN notation. Figure 10 illustrates the basic steps by means of a flow chart.

The circuit shown in Fig. 11(a) will be used to demonstrate the procedure. The nodes, branches, positive current directions, and output are designated. Positive voltages are understood to oppose the current arrows. Part (b) of the

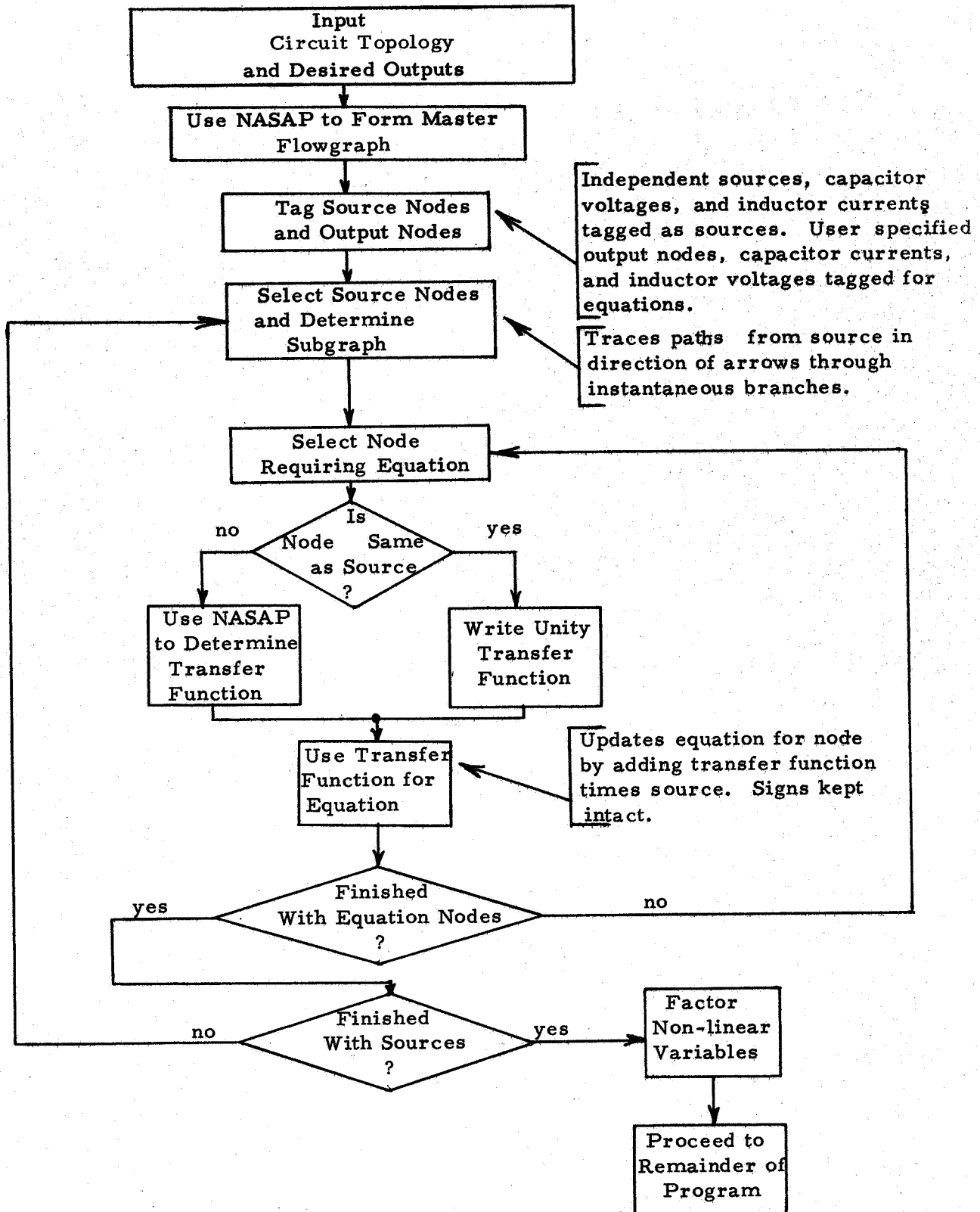
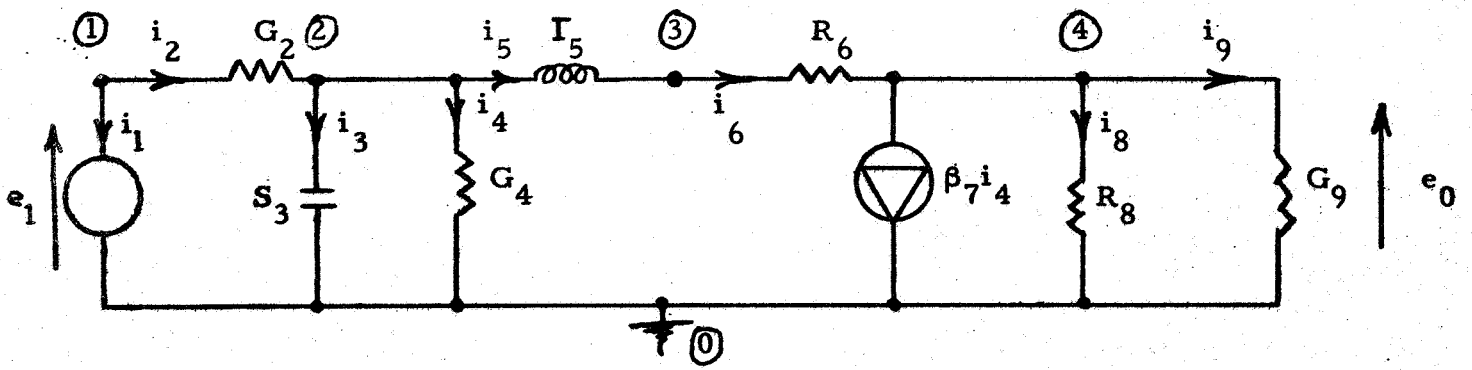
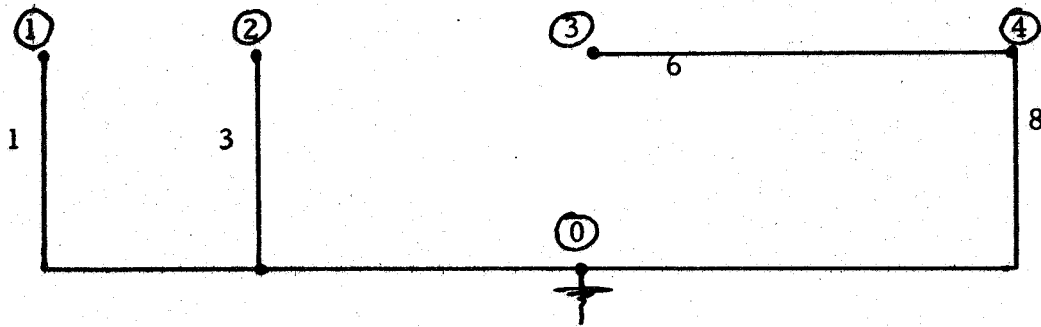


Fig. 10 BASIC STEPS IN PART 1.



(a) Circuit



(b) Tree

(branch)	(nodes)	(element)	(controlled by branch)
1	(1, 0)	V1	
2	(1, 2)	G2F	
3	(2, 0)	S3	
4	(2, 0)	G4F	
5	(2, 3)	T5F	
6	(3, 4)	R6F	
7	(4, 0)	B7F	4
8	(4, 0)	R8	
9	(4, 0)	G9	

V9 = ?

(c) Input to Part 1.

Fig. 11 SAMPLE ANALYSIS

illustration indicates the tree which the program will use. It is advisable for the user to determine a tree in order to see if the circuit is acceptable.

Figure 11(c) indicates the program input. The letter "F" in an element designation indicates that the user will employ a function in describing the element behavior. The letter "F" is not used in conjunction with independent sources (V1) nor with linear elements (R8, G9).

Observe that element G2 can be nonlinear since it is in a loop consisting of independent voltage sources and capacitors. The same is true for G4. Element R6 can be nonlinear since it is in a cut-set with the inductor. Also, B7 can be nonlinear since the argument i_4 is associated with a resistor that is in a capacitor loop. Capacitors and inductors can always be nonlinear. A linear capacitor and a nonlinear conductor are designated. The resistors R8 and G9 must be linear. The input specifies an additional equation for V9.

The first step is to form the master flowgraph. This is illustrated in Fig. 11. The source nodes are solid and the nodes requiring equations are

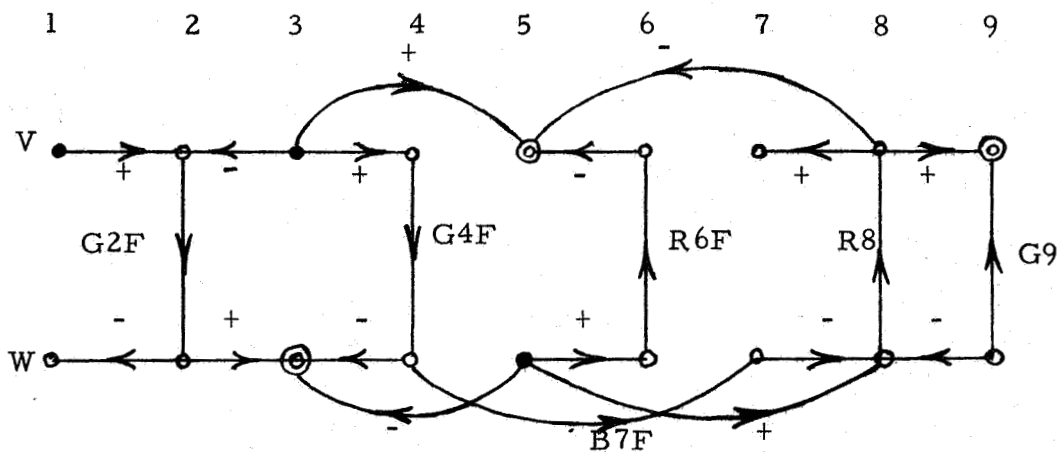


Fig. 12 MASTER FLOWGRAPH

tagged by double circles. Observe that the capacitor and the inductor are regarded as sources.

The first step is to select a source and determine the subgraph affected by the source. The subgraph is obtained by tracing the arrows beginning at the source. For example, Fig. 13 illustrates the subgraph corresponding to source V1. The equations resulting from the application of the closed loop

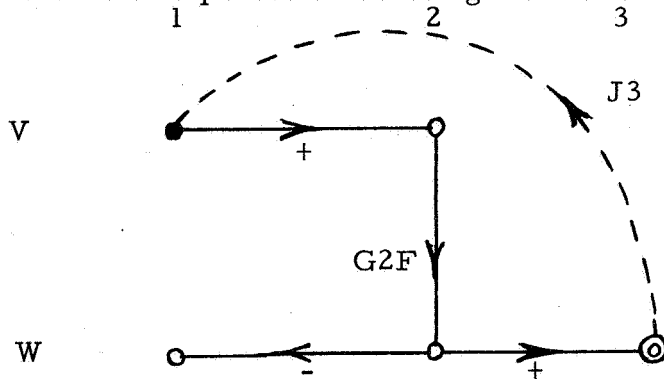


Fig. 13 SUBGRAPH FOR V1

thus far:

$$W3 = +G2F (+V1) \dots$$

$$V5 = \dots$$

$$V9 = \dots$$

The quantities V5 and V9 are not directly affected by V1.

Figure 14 indicates the subgraphs for both of the remaining sources.

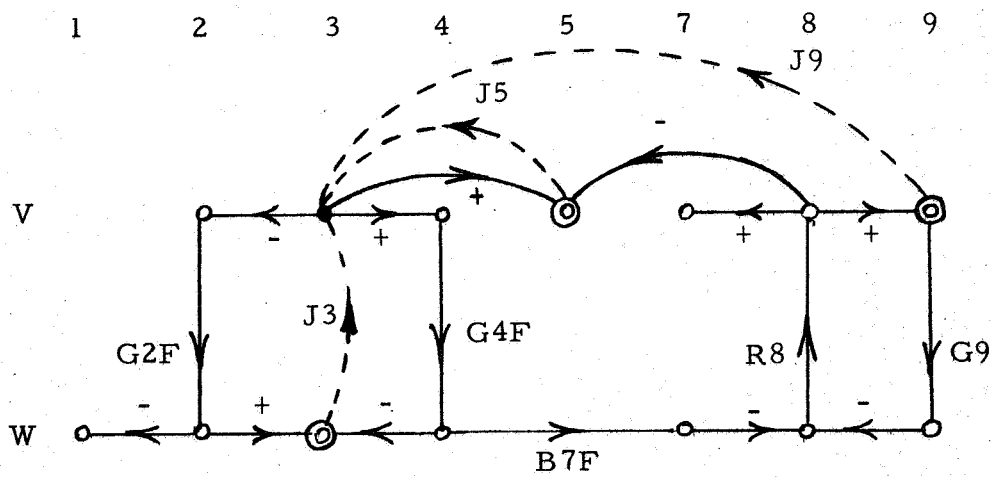
Unlike Fig. 13, the subgraphs in Fig. 14 must each be used several times. The reason for this is that the sources appear explicitly in more than one equation.

The updated equations determined from Fig. 14(a) are:

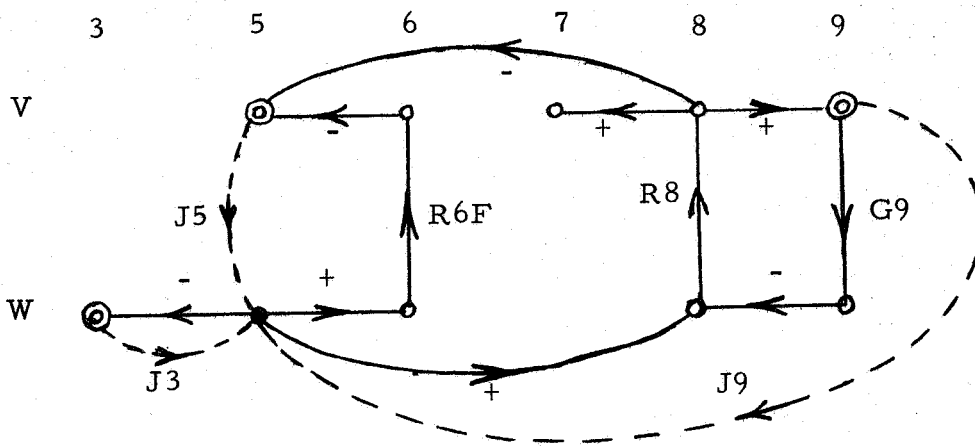
$$W3 = +G2F(+V1) + G2F(-V3) - G4F(+V3) \dots$$

$$V5 = (+V3) - (R8/(1+R8*G9)) * (-B7F(+G4F(+V3))) \dots$$

$$V9 = (R8/(1+R8*G9)) * (-B7F(+G4F(+V3))) \dots$$



(a) Source V3



(b) Source W5

Fig. 14 REMAINING SUBGRAPHS

The complete equations follow:

$$\begin{aligned}
 W3 &= +G2F(+V1) + G2F(-V3) - G4F(+V3) - W5 \\
 V5 &= (+V3) - (R8/(1+R8*G9)) * (-B7F(+G4F(+V3))) \\
 &\quad - R6F(+W5) - (R8/(1+R8*G9)) * (+W5) \\
 V9 &= (R8/(1+R8*G9)) * (-B7F(+G4F(+V3))) \\
 &\quad + (R8/(1+R8*G9)) * (+W5)
 \end{aligned}$$

The remaining operations are factorization for "function call" arguments and reduction of signs and parentheses. The state and output equations of part 1 are:

$$\begin{aligned}
W3 &= G2F(V1 - V3) + G4F(V3) - W5 \\
V5 &= V3 - (R8/(1+R8*G9)) * (-B7F(G4F(V3))) \\
&\quad - R6F(W5) - (R8/(1+R8*G9)) * W5 \\
V9 &= (R8/(1+R8*G9)) * (-B7F(G4F(V3))) \\
&\quad + (R8/(1+R8*G9)) * W5
\end{aligned}$$

The first part will provide other FORTRAN statements which are essential for the arithmetic computations in part 2. An example of these statements is indicated for integration in the succeeding section.

4.4 Integration

If a time response of the output is desired by the user, then part 2 will utilize the equations of part 1 for integration. An integration routine has not yet been selected. It will most likely be the "Adams" method⁴⁴ of about the fourth order. The user will be required to select the time increment, duration of computation, and number of output points desired. The increment will be varied about the user selected value according to the curvature of the function.

In addition to the preceding, the user will be required to specify the initial charge on all capacitors and the initial flux linkages for all inductors. The circuit elements will also be defined by either constants or FORTRAN functions. Table IV indicates the arrangement of the cards (or FORTRAN statements) which constitute the input to part 2 of the program.

The arrangement of statements corresponding to the preceding example follows.

```

T $\phi$  = 0. (initial time)
TF = 1. E-6 (final time)
DT = 1. E-9 (time increment)
NP = 100 (no. output points)
Q3 = 5. (initial charge)
F5 = 7. (initial flux linkage)
G2F(V2) = (1. E-6) * EXPF (39. *V2)
S3 = 1. / (1. E-6)
G4F(V4) = (1. E-7) * EXPF (39. *V4)
T5F(F5) = F5 / .001 + F5 * ABSF (F5)
R6F(W6) = (100. + 10. ABSF (W6)) * W6
B7F(W4) = 100. * W4 * EXPF (- .1 * ABSF (W4))
R8 = 100.
G9 = 1. / 1000.
DIMENSION W3I(n), V5I(n)
D $\phi$  100 J = 1, n
W3I(J) = 0.
V5I(J) = 0.
100  C $\phi$ NTINUE
T = T $\phi$ 
200  C $\phi$ NTINUE
V3 = S3 * Q3
W5 = T5F(F5)
V1 = 10. * SINF(7. * T)
W3 = ~~~~~
V5 = ~~~~~
V9 = ~~~~~
D $\phi$  300 J = 1, n-1
W3I(J) = W3I(J + 1)
V5I(J) = V5I(J + 1)
300  C $\phi$ NTINUE
W3I(n) = W3
V5I(n) = V5
Q3 = INT (Q3, W3I(1), ..., W3I(n), DT)
F5 = INT (Q3, V5I(1), ..., V5I(n), DT)
T = T + DT
IF(T-TF) 200, 200, 400
400  C $\phi$ NTINUE
END

```

(USER SUPPLIED.)

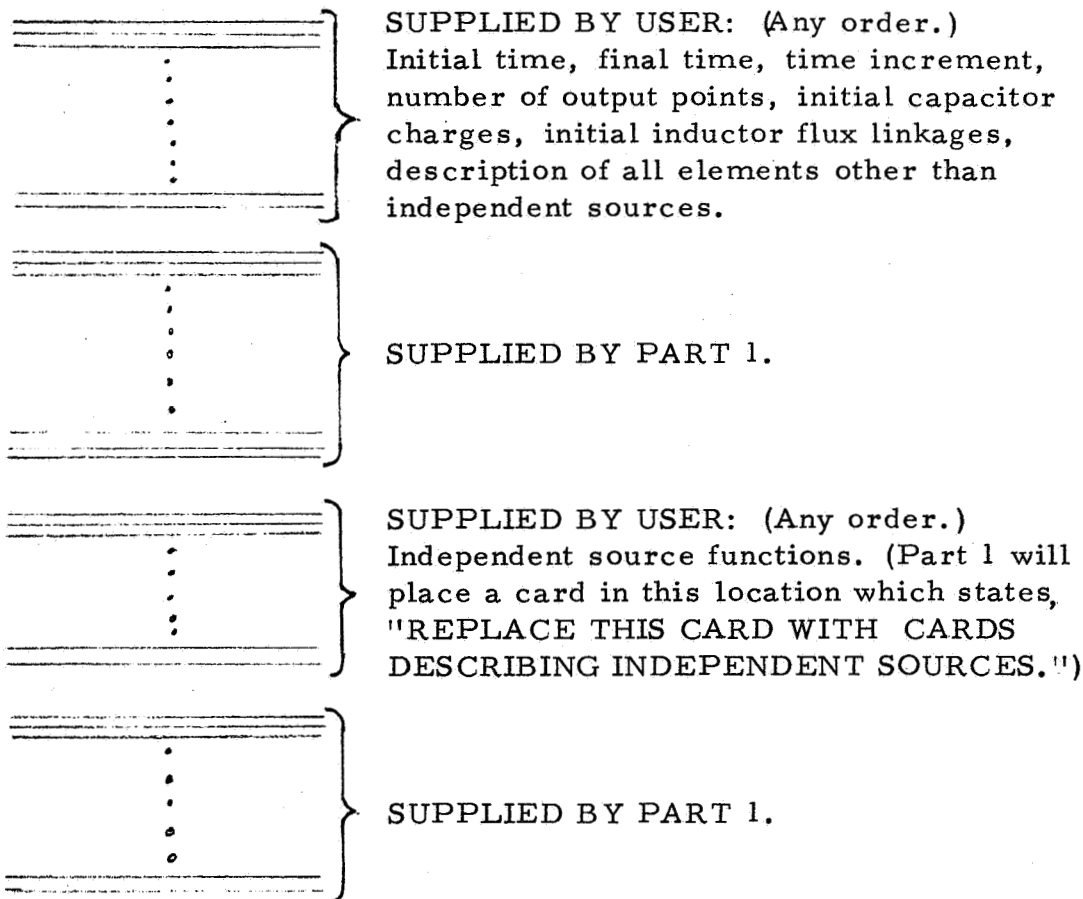
(SUPPLIED BY PART 1.)

(USER SUPPLIED.)

(REMAINDER SUPPLIED
BY PART 1.)

TABLE IV

Arrangement of Cards for Part 2



The FORTRAN statements used for the circuit elements correspond to the following:

$$f_{G2}(v_2) = 10^{-6} \epsilon^{39v_2}$$

$$S_3 = 1/10^{-6}$$

$$f_{G4}(v_4) = 10^{-7} \epsilon^{39v_4}$$

$$f_{I5}(\lambda_5) = \frac{\lambda_5}{.001} + \lambda_5 |\lambda_5|$$

$$f_{R6}(i_6) = (100 + 10 |i_6|) i_6$$

$$f_{\beta 7}(i_4) = 100i_4 \epsilon^{-.1|i_4|}$$

$$R_8 = 100$$

$$G_9 = 1/1000$$

$$v_1(t) = 10 \sin(7t)$$

The quantity "n" corresponds to the order used in the integration routine. For a fourth order, n=4. The subprogram designated by "INT" represents the integration routine. The above statements exclude provisions for the computer output and the adjustment of the time increment. Figure 15 indicates the flow chart for part 2 of the program.

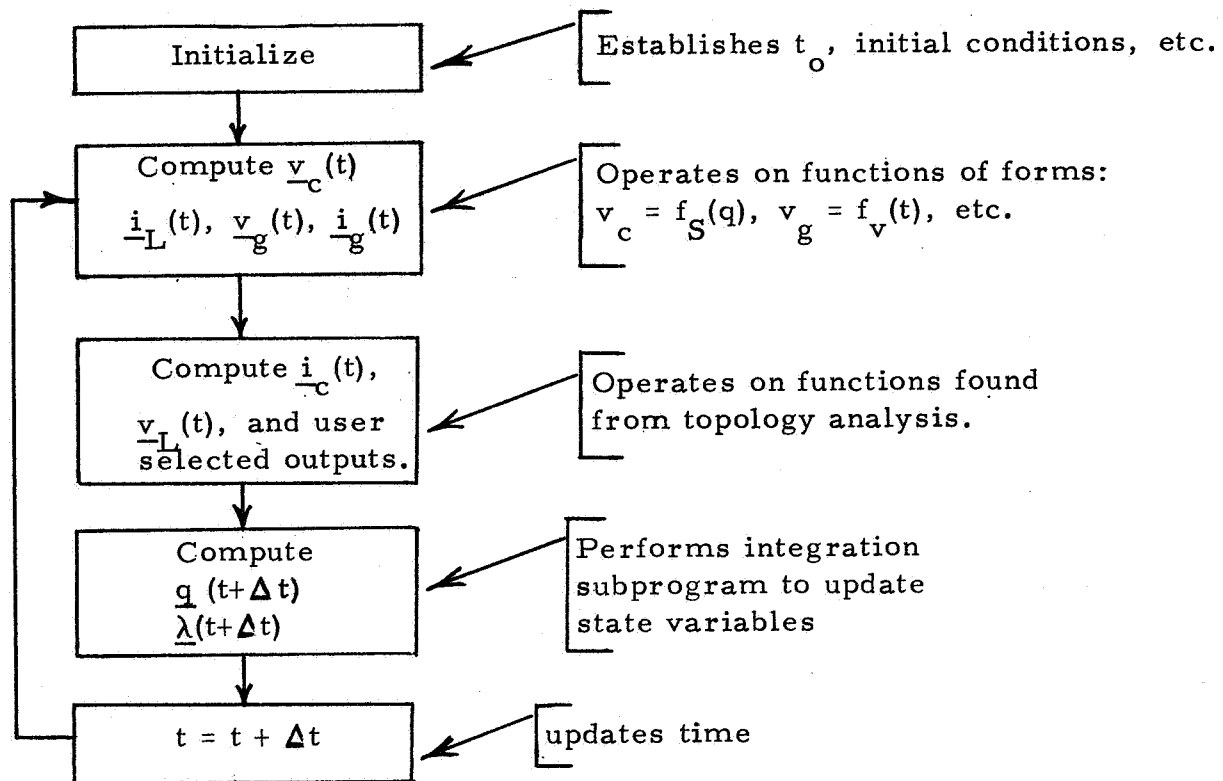


Fig. 15 FLOWCHART FOR PART 2

5. SUMMARY AND CONCLUSIONS

Modeling procedures and analytical techniques have been developed for the prediction of microcircuit failure modes when these devices are operated under adverse environmental conditions. A systematic procedure, based upon the Linvill lumped-parameter representation, has been employed in deriving microcircuit models directly from structure, material properties, and known radiation and thermal effects. This modeling procedure was used to obtain the lumped-parameter representation of a typical microcircuit device. The NASAP program was then used to analyze the response of a linear microcircuit under the effects of radiation.

Diagnostic techniques, based upon the statistical tolerance calculated from sensitivity functions, have been developed. These techniques have been applied to the formulation of design procedures for microcircuits which are insensitive to adverse environmental effects. Two related design formulations are presented which are to be developed more fully during continued research in this area.

A nonlinear version of the NASAP computer program is presented, based on the fundamental principles of the linear NASAP program. In addition to a description of the basic program, algorithms for sensitivity and worst-case analyses of nonlinear networks are presented as the basis for the development of diagnostic techniques for microcircuits operated in a nonlinear mode. Application of the nonlinear program to nonlinear Linvill lumped-parameter models of semiconductor devices is demonstrated.

It is concluded from this research that:

1. Environmental effects on microcircuits may be described accurately with the use of the Linvill lumped-parameter modeling technique. This technique allows direct connection between the cause and response of an environmental effect in the region of the device which is most sensitive.
2. The network-like elements of the lumped-parameter model allow for the application of flowgraph theory for analysis. The NASAP program, based on flowgraph analysis, is quite suitable for failure mode diagnostics of microcircuits.
3. Design procedures, based upon a statistical tolerance formulation, may be used to obtain the least sensitive element values of a network with the aid of the NASAP program.
4. Nonlinear network elements and the Linvill lumped-parameter representation of microcircuits operating in a nonlinear mode may be analyzed using a modified version of the NASAP program.

REFERENCES

1. R. A. Smith, Semiconductors, Cambridge Press, London, 1961.
2. J. F. Gibbons, Semiconductor Electronics, McGraw-Hill, New York, 1966.
3. G. Wertheim, "Radiation Effects in Semiconductors," pp. 46-52, Nucleonics, Vol. 20, No. 7, July, 1962.
4. G. C. Messenger, "Radiation Effects on Microcircuits," 1966 Radiation Effects Conference, Palo Alto, July, 1966.
5. W. W. Happ and H. Potash, "Modeling Procedures for Interactions Between Thermal and Electrical Device Parameters," Solid State Electronics, September, 1966.
6. Batelle Memorial Institute, 1966 TREE Handbook, Sections F and G.
7. J. J. Ebers and J. L. Moll, "Large Signal Behavior of Junction Transistors," Proc. IRE, Vol. 42(12), 1761-72, December, 1954.
8. R. Beaufoy and J. J. Sparkes, "The Junction Transistor as a Charge Controlled Device," ATE Journal, Vol. 13, 310-27, Oct., 1957.
9. J. G. Linvill, "Lumped Models of Transistors and Diodes," Proc. IRE, Vol. 46, No. 6, pp. 949-962, June, 1958.
10. G. J. Herskowitz, "Modeling Integrated Circuits for Computing," National Electronics Conference Proceedings, Vol. 23, pp. 199-203, October, 1967.
11. G. J. Herskowitz, et. al., Computer-Aided Integrated Circuit Design, McGraw-Hill, New York, 1968.
12. F. H. Branin, Jr., et. al., Proc. IEEE Special Issue on Computer-Aided Design, Vol. 55, No. 11, pp. 1775-2072, November, 1967.
13. R. M. Carpenter and W. W. Happ, "Symbolic Approach to Computer-Aided Design," Electronics, Vol. 39, No. 25, pp. 92-98, December, 1966.
14. S. J. Mason and H. J. Zimmerman, Electronic Circuits, Signals and Systems, John Wiley, New York, 1960.
15. W. W. Happ and J. B. Compton, "Flowgraph Models of Integrated Circuits and Film-Type Systems," IEEE Trans. on Aerospace, AS-2, pp. 259-271, April, 1964.

16. W. W. Happ, "Modeling of Integrated Semiconductor Structures," Southwest IEE Conference, Dallas, Texas, April 22, 1964.
17. W. W. Happ and J. B. Compton, "Modeling of Radiation Effects in Semiconductor Devices and Circuits," IEEE Trans. on PTG-Aerospace, Vol. AS-3, No. 2, pp. 372-378, June, 1965.
18. W. W. Happ and D. E. Moody, "Topological Techniques for Sensitivity Analysis," IEEE Trans. PG-ANE-11, No. 4, pp. 228-254, December, 1964.
19. T. J. Kobylarz, "The Application of the NASAP Program in the Analysis of Nonlinear Networks," NASA Progress Report submitted to the Electronics Research Center, Cambridge, Mass., October, 1966.
20. G. J. Herskowitz and T. J. Kobylarz, "Computer Analysis of Networks with Nonlinear Linvill Elements," to be published.
21. W. Shockley and W. T. Read, Jr., "Statistics of the Recombinations of Holes and Electrons," Phys. Rev., Vol. 87, pp. 835-842, 1952.
22. J. Bardren and W. Shockley, "Deformation Potentials and Mobilities in Nonpolar Crystals," Phys. Rev. 80, 72; October, 1950.
23. H. Brooks, "Scattering by Ionized Impurities in Semiconductors," Phys. Rev. 83, 879(A), August, 1951.
24. J. Warner and J. Fordemwalt, Integrated Circuits, McGraw-Hill, N. Y. pg. 178, 1965.
25. W. W. Gartner, Transistors: Principles, Design and Applications, pg. 87, 1960.
26. D. G. Mark and L. H. Stember, "Variability Analysis," Electro-Technology, pp. 37-48; July, 1965.
27. G. J. Herskowitz, "Active RC Filter Design by Computer," Chapter VI of Computer-Aided Network Design, edited by G. Zobrist, Boston Technical Publishers, Massachusetts, 1968.
28. G. J. Herskowitz, "An Integrated Gated Differential Amplifier for High Speed Variable Memory Digit Detectors," 1965 International Solid-State Circuits Conference Technical Digest, February, 1965.
29. D. C. Sowin, et. al., "Microcircuit Hardening Study," presented at IEEE Annual Conference on Nuclear and Space Radiation Effects, Stanford University, Palo Alto, California, July, 1966.

30. O. L. Curtis, Jr., "Effects of Oxygen and Dopant on Lifetime in Neutron Irradiated Silicon," *ibid.*
31. G. J. Herskowitz, "Automated Design of Networks Within Specified Response and Impedance Constraints," to be published.
32. E. Zeheb, "Simplified Integrated Circuit Filter Design with Computer Oriented Optimization," to be published.
33. E. A. Guillemin, *Synthesis of Passive Networks*, John Wiley and Sons, Inc., pp. 141-157, 1957.
34. J. D. Schoeffler, "Synthesis of Minimum Sensitivity Networks," IEEE Trans. on Circuit Theory, Vol. 11, No. 2, pp. 271-276, June, 1964.
35. K. L. Su, "Active Network Synthesis," McGraw-Hill, 1965.
36. R. W. Newcomb, T. N. Rao and J. Woodard, "A Minimal Capacitor Cascade Synthesis for Integrated Circuits," *Microelectronics and Reliability*, Vol. 6, 1967, pp. 113-124.
37. O. Brune, "Synthesis of a Finite Two-terminal Network Whose Driving-point Impedance is a Prescribed Function of Frequency," *J. Math and Phys.*, Vol. 10, 1931, pp. 191-236.
38. A. G. J. Holt and J. Taylor, "Method of Replacing Ungrounded Inductors by Grounded Gytrators," *Electron. Lett.*, Vol. 1, 1965.
39. I. Navot and E. Zeheb, "Two Theorems on Hurwitz Polynomials and Their Applications to Symmetrical and Antimetric Two-Ports," *IEEE Trans. on Circuit Theory*, Vol. CT-11, Dec., 1964.
40. I. Navot, "On the Bisection of Symmetric and Antimetric Reactance Two-Ports," *IEEE Trans.*, Vol. CT-12, Dec., 1965.
41. Carpenter, R. 1967. NASAP: Network Analysis for Systems Applications Program: Present Capabilities of a Maintained Program. Computer Aided Circuit Design Seminar sponsored by NASA ERC, Cambridge, Mass.
42. Carpenter, R. and Happ, W. W. 1966a. Computer Aided Circuit Design: Part 3 Analyzing Circuits With Symbols. *Electronics*, 39:25:92-98.
43. Carpenter, R. and Happ, W. W. 1966b. Algorithms for the dichotomous representation of macrocircuits. *Proc. Fourth Annual Allerton Conf. on Circuit and System Theory.*

APPENDIX A: ACTIVE RC FILTER TRANSFER FUNCTION AND SENSITIVITY ANALYSIS USING NASAP

The NASAP program will be employed to systematically analyze low- and high-pass active RC filter sections by computer and perform sensitivity analyses. Take as an example the filter design specifications given in Fig. A-1.

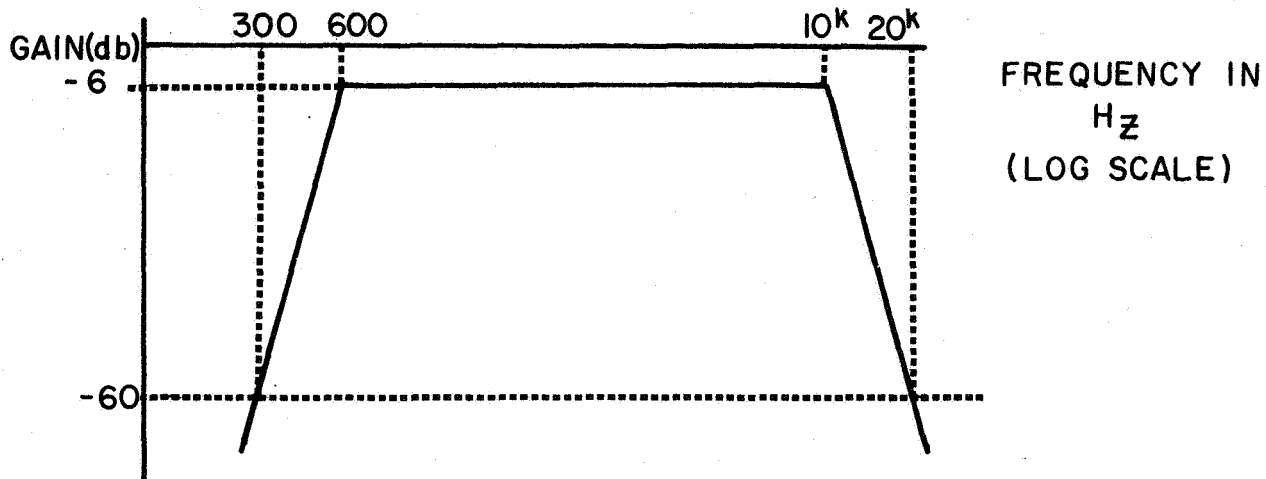


Fig. A-1
Ripple in Pass Band 1.5 db
Input-Output Impedance -600 Ω

To achieve the steep rolloff outside the passband a Chebyshev filter will be employed in the design. The Butterworth filter requires more sections for the same amount of selectivity. The number of sections needed is found from the rolloff requirement to be seven for both the low- and high-frequency skirts (down 60 db an octave from the corner frequencies). The low- and high-pass filter sections will be designed for 0.5 db ripple to satisfy the 1.5 db overall ripple requirement in the pass band. A 7-pole Chebyshev filter section needed to realize the skirt selectivity within the ripple requirement has pole

locations shown below in Figure A-2.

$$S_1 = -0.256$$

$$S_{2,3} = -0.057 \pm j 1.006$$

$$S_{4,5} = 0.160 \pm j 0.807$$

$$S_{6,7} = -0.231 \pm j 0.448$$

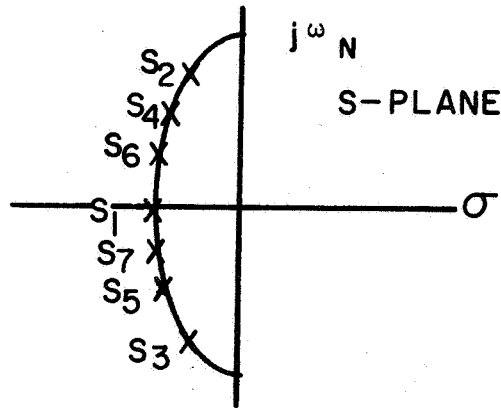


Fig. A-2

Each pair of complex poles may be realized by one active RC filter stage. The single pole at S may be realized with a passive RC section. Each pair of complex poles may be written in the normalized form

$$S_n = -\sigma + j\omega_c \tag{A-1}$$

The voltage transfer function corresponding to the pair of poles is

$$T(S_n) = \frac{H}{S_n^2 + 2\sigma S_n + \omega_n^2} \tag{A-2}$$

where

$$\omega_n^2 = \sigma^2 + \omega_c^2$$

H = arbitrary gain constant

Since the transfer function of (24) is normalized to ω_{3db} , it is necessary to denormalize by using the transformation

$$S = \omega_{3db} S_n \tag{A-3}$$

Performing this denormalization results in the low- and high-pass filter section transfer functions given in Table A-1.

Table A-1

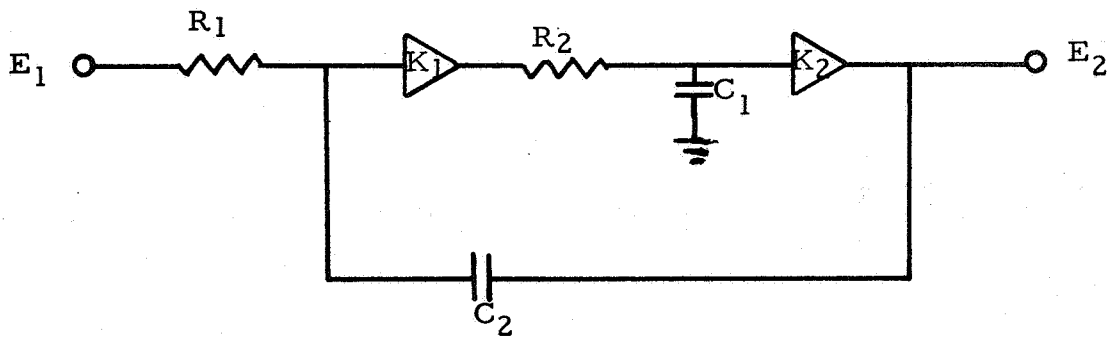
<u>Low - Pass</u>	<u>High - Pass</u>
$T_{1L}(S) = \frac{H_{1L}}{S + 0.249}$	$T_{1H} = \frac{H_{1H} S}{S + 4.02}$
$T_{2L}(S) = \frac{H_{2L}}{1.044S^2 + 0.116S + 1}$	$T_{2H} = \frac{H_{2H} S}{0.958S^2 + 0.111S + 1}$
$T_{3L}(S) = \frac{H_{3L}}{1.57S^2 + 0.49S + 1}$	$T_{3H}(S) = \frac{H_{3H} S^2}{0.54S^2 + .31S + 1}$
$T_{4L}(S) = \frac{H_{4L}}{4.18S^2 + 1.87S + 1}$	$T_{4H}(S) = \frac{H_{4H} S^2}{0.24S^2 + 0.45S + 1}$

The constant H multipliers are determined from the circuit realization procedure employed. For active RC network realization, the constant H multipliers are related to the amplifier gains and RC time constants of the circuit. In this case, the circuit of Fig. A-3 will be used to realize the low-pass section and that of Fig. A-4, the high-pass section.

Comparing the poles of the low- and high-pass sections in Table A-1 with the transfer functions described by the equations below Figs. A-3 and A-4 results in the following values of τ , the RC time constants.

Table A-2

Low-Pass Sections				High-Pass Sections			
T_{1L}	T_{2L}	T_{3L}	T_{4L}	T_{1H}	T_{2H}	T_{3H}	T_{4H}
$\tau = 0.249$	$\tau_1 = 9.04$ $\tau_2 = 0.12$	$\tau_1 = 3.22$ $\tau_2 = 0.486$	$\tau_1 = 2.23$ $\tau_2 = 1.87$	$\tau = 4.02$	$\tau_1 = 0.12$ $\tau_2 = 8.65$	$\tau_1 = 0.31$ $\tau_2 = 2.06$	$\tau_1 = 0.45$ $\tau_2 = 0.51$

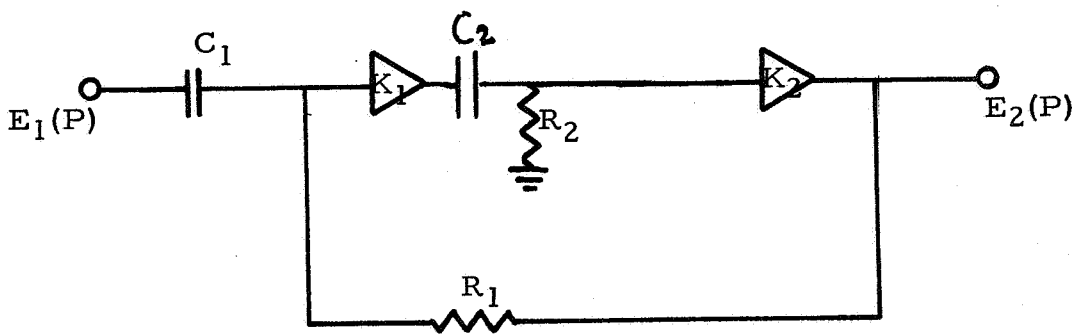


$$\tau_1 = R_1 C_1$$

$$\tau_2 = R_2 C_2$$

Fig. A-3 Low-Pass Active RC Filter Section

$$\frac{E_2(S)}{E_1(S)} = \frac{\frac{K_1 K_2}{\tau_1 \tau_2}}{S^2 + \frac{\tau_2 + (1 - K_1 K_2) \tau_1}{\tau_1 \tau_2} S + \frac{1}{\tau_1 \tau_2}}$$



$$\tau_1 = R_1 C_1$$

$$\tau_2 = R_2 C_2$$

Fig. A-4 High-Pass Active RC Filter Section

$$\frac{E_2(S)}{E_1(S)} = \frac{K_1 K_2 S^2}{S^2 + \frac{\tau_1 + (1 - K_1 K_2) \tau_2}{\tau_1 \tau_2} S + \frac{1}{\tau_1 \tau_2}}$$

Considering the high-pass section T_{2H} , choosing $H = 1$, the coded equivalent circuit and input matrix for the NASAP program are given in Fig. A-5 and Table A-3 respectively. Note that element 8 has been added to the circuit to effect closure and element 2, a very large resistance, has been added to develop a voltage across the input of amplifier K_1 which can be labelled as a voltage between two vertices of the equivalent circuit.

Fig. A-5

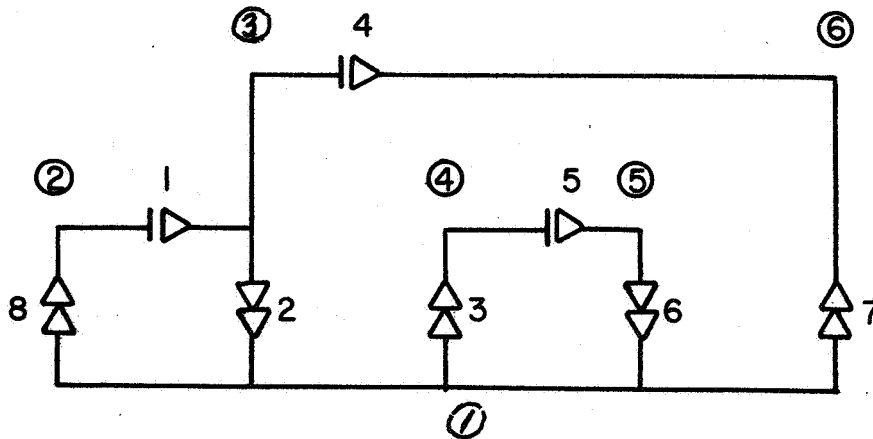


Table A-3

A	B	C	D	E	F	G	H	K	Numerics
2	3	0	1	1	1	1	0	0	.499E - 8
3	1	1	2	2	0	0	0	0	.500E + 10
1	4	0	2	3	0	0	0	1	.100E + 1
3	6	0	4	4	0	1	0	0	.169E - 3
4	5	0	5	5	1	1	0	0	.399E - 7
5	1	1	6	6	0	0	0	0	.573E + 5
1	6	0	6	7	0	0	0	0	.100E + 1
1	2	0	7	8	0	0	1	0	.100E + 1

The encoding of the circuit is as follows:

- (1) Elements 1 and 5 are capacitors C_1 and C_2 taken as admittances (voltage controlled current sources). Their frequency dependence is therefore +1.
- (2) Elements 3 and 7 are amplifiers K_1 and K_2 having unity gain with no frequency dependence.
- (3) Elements 4 and 6 are resistors R_1 and R_2 taken as an admittance and impedance respectively. They are frequency independent.
- (4) Element 8, which has been added for closure, is tagged with a +1 in column K_1 .
- (5) Element 3, amplifier K_1 , is tagged in the sensitivity column. The computer will therefore calculate the sensitivity of transfer function T_{2H} to gain K_1 .

In addition to verifying and producing a Bode plot (Fig. 6) of the transfer function T_{2H} , the sensitivity function $S_{K_1}^{T_{2H}}$ is listed by the computer:

$$S_{K_1=1}^{T_{2H}} = - \frac{(.33E+0) S^2 + (.11E+5) S + (.49E+7)}{(.33E+0) S^2 + (.14E+3) S + (.49E+7)}$$

Since $S_{K_1=1}^{T_{2H}}$ is a function of frequency, a significant point to examine this function is at $\omega_{3db} = 2\pi \times 10^4$ /sec. This results in a sensitivity function $S_{K_1=1}^{T_{2H}} = -1.52$.

Fig. A-6 (a)

Bode Plot Log |T_{2H}| V_S Log ω

YMIN= -.99999999+02

YMAX= .00000

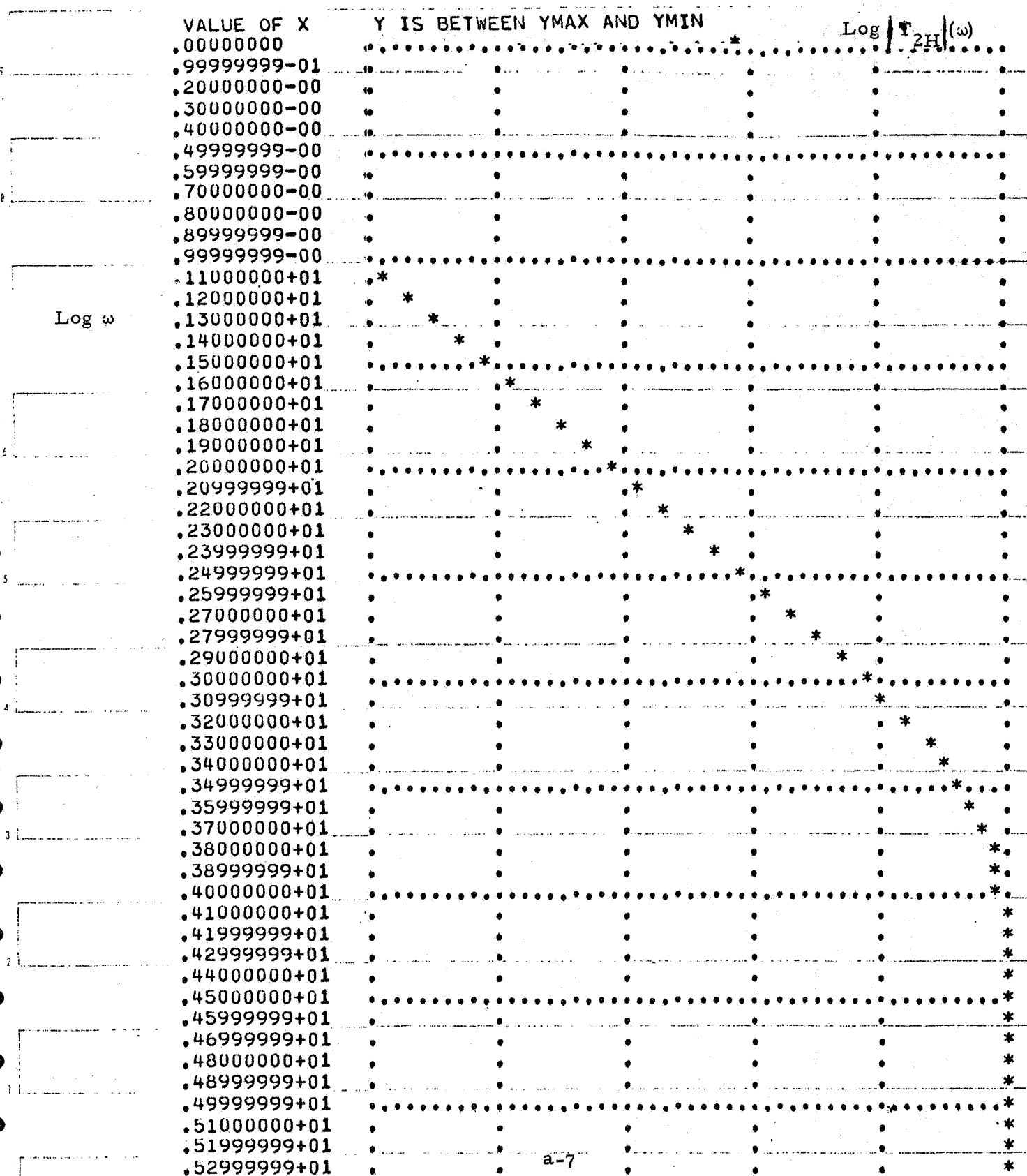
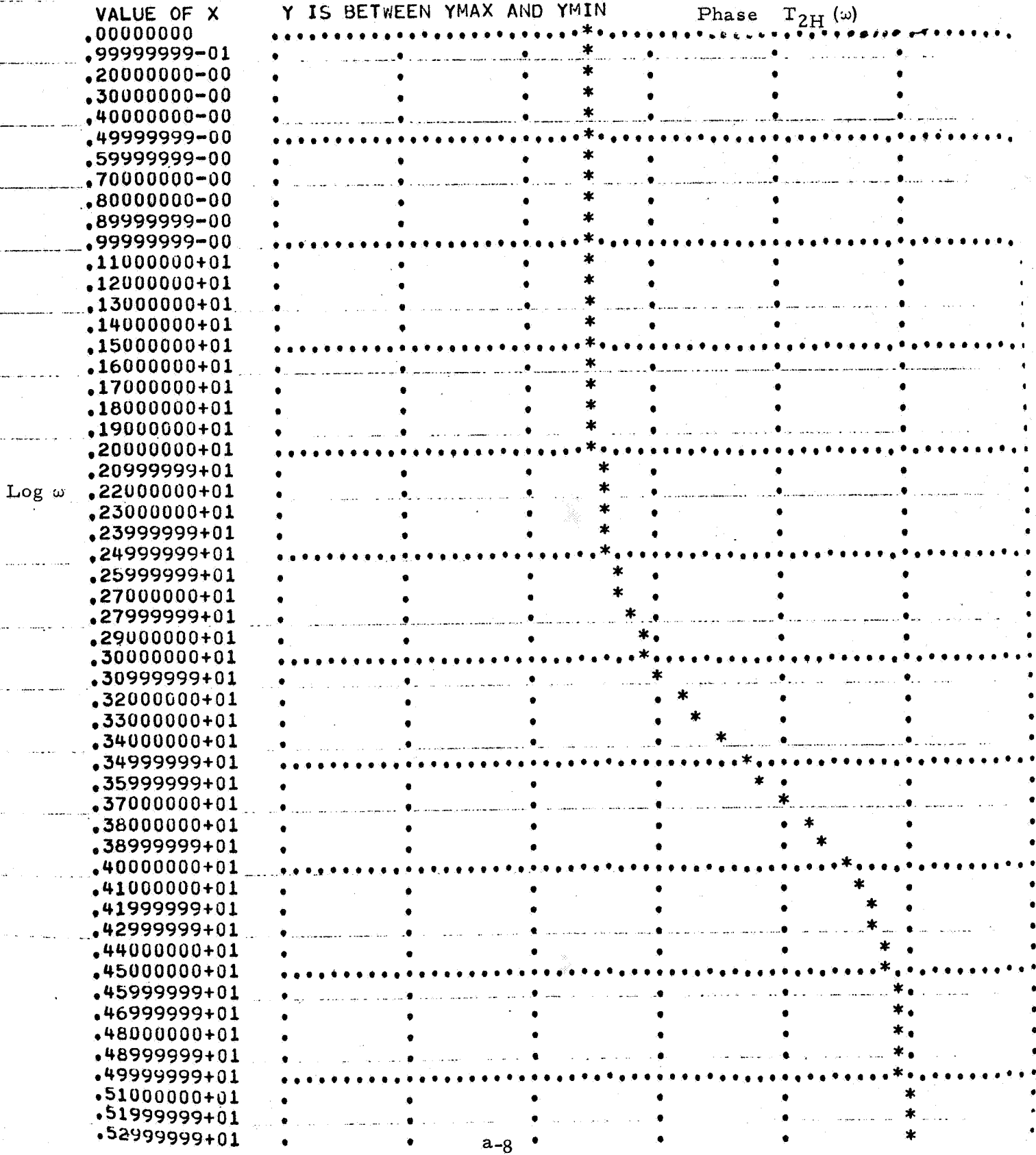


Fig. A-6 (b)

Bode Plot Phase T_{2H} V_S $\text{Log } \omega$

YMIN= -.18000000+03

YMAX= .18000000+03



APPENDIX B: ANALYSIS OF LINEAR INTEGRATED CIRCUITS UNDER THE EFFECTS OF RADIATION USING THE LINVILL MODEL

The operation of a typical linear integrated circuit in a radiation environment will be analyzed using the Linvill lumped-parameter model. The circuit selected for study is the differential amplifier configuration (Fig. B-1) which is a part of many commercially available integrated circuits.²⁴ It is used to achieve balanced gain in systems where noise and thermal effects are significant factors.²⁸ In the radiation environment, this circuit may be used to minimize transient radiation disturbances.²⁹ Both permanent damage and transient radiation effects will be considered in the analysis of this circuit.

It will be assumed for the purpose of this illustration that the integrated circuit transistors employed in the amplifier of Fig. B-1 have been fabricated in the configuration of Fig. 4, resulting in the Linvill parameters derived in Section 2.2, and interconnected in the manner of Fig. 6. Permanent radiation damage is primarily the result of high energy particles which degrade the effective carrier lifetime according to Eq. (7). Measurements have been made on N- and P-type silicon to determine the value of damage constant K at low injection levels as a function of resistivity.³⁰ Using an average material resistivity of 10Ω - cm, K is 1.5×10^5 pvt-sec. for N-material and 3.5×10^{15} pvt-sec. for P-material.

The effect of lifetime degradation may be included in the Linvill model of Fig. 6 through the "combinance" parameters, H_{cE} , H_{cI} , H_{cB} , and H_{cC} . These parameters are related to "storance" S and lifetime τ through Eq. (8). Also, since the current through the combinance is proportional to the excess charge density, it is convenient to write the recombination current in terms of S and τ ;

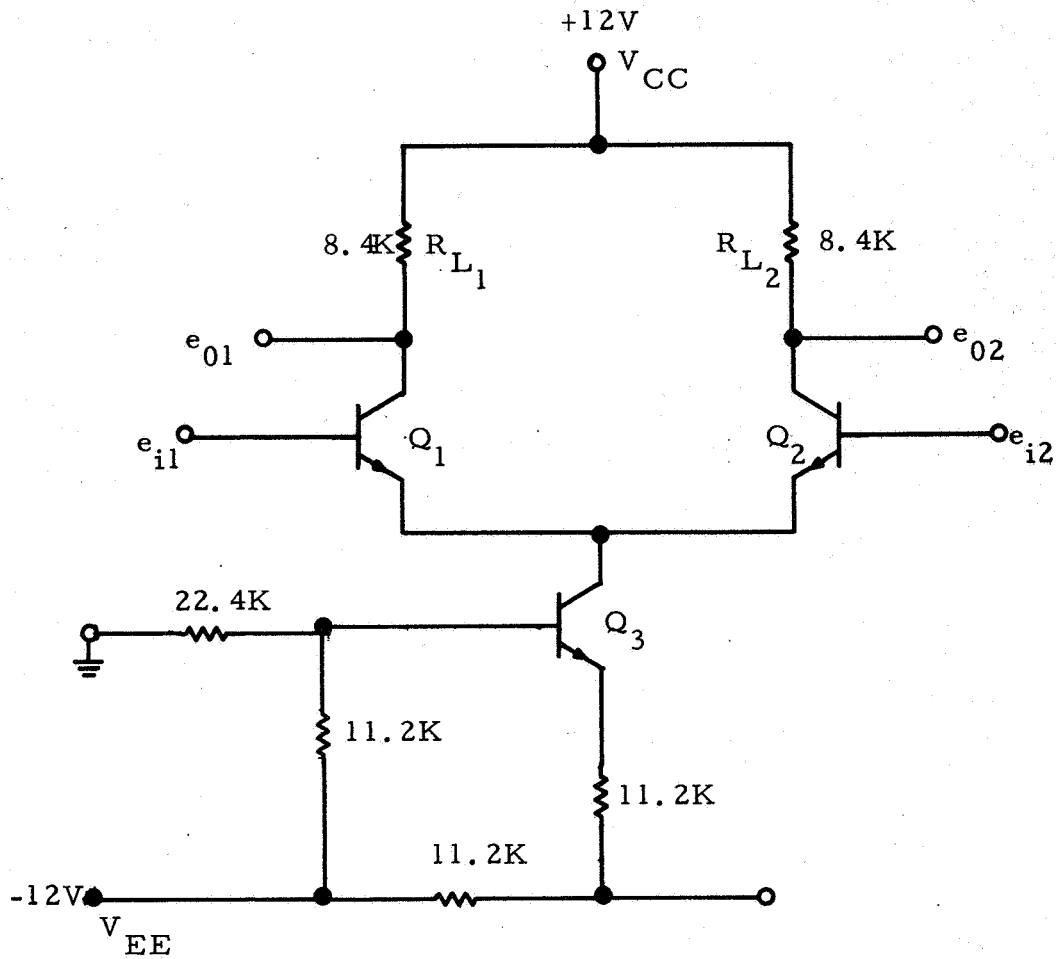


FIG. B-1 DIFFERENTIAL AMPLIFIER INTEGRATED CIRCUIT

$$i_{nr} = H_{nc} (Q_n - Q_{no}) = \frac{S_n}{\tau_n} (N_p - N_{po}) \quad (B-1)$$

in the base region. Since the emitter region of a high frequency transistor is much more heavily doped than the base or collector regions,²⁴ it behaves as a good conductor, and the charge storage and recombination effects, described by S_E and H_{cE} , may be ignored in the model.

The minority carrier densities at the edges of the emitter and collector depletion regions are related to the equilibrium carrier densities according to the expressions, derived from Eq. (18),

$$P_E = P_{nE} \exp. \left(q \frac{V_{EB}}{kT} \right) \quad (B-2)$$

$$N_E = N_{pB} \exp. \left(q \frac{V_{EB}}{kT} \right) \quad (B-3)$$

$$N_c = N_{pE} \exp. \left(q \frac{V_{cB}}{kT} \right) \quad (B-4)$$

$$P_c = P_{nc} \exp. \left(q \frac{V_{cB}}{kT} \right) \quad (B-5)$$

where

P_{ne} = equilibrium hole density in emitter region

N_{pb} = equilibrium electron density in base region

N_{pe} = equilibrium electron density in collector region

P_{nc} = equilibrium hole density in collector region.

During normal active operation of the transistor, the emitter-base junction is forward-biased, and the collector-base junction is reverse-biased. A reverse bias of more than one volt causes N_c and P_c of Eqs. (B-4) and (B-5) to be much smaller than P_E and N_E . The usual approximation under this condition is to

neglect variation of charge beyond H_D in the base region, assuming it is collected unchanged at the collector terminal.⁸ In addition, for small-signal a. c. operation, Eqs. (B-2) and (B-3) may be approximated by

$$P_e = dP_E \approx \frac{q}{kT} P_E v_{eb} \quad (B-6)$$

and

$$n_e = dN_E \approx \frac{q}{kT} N_E v_{eb} \quad (B-7)$$

where v_{eb} , P_e , and n_e are the small-signal a. c. voltage and charge associated with the emitter-base junction.

The lumped-parameter model of the integrated circuit transistor may be represented, as a result of these approximations, by the equivalent circuit of Fig. B-2 which includes a transient radiation generator in the base region. The integrated circuit resistors may be modeled for linear operation over a narrow frequency range by a lumped resistor with a single capacitance to the substrate of about 1 pf, illustrated in Fig. B-3. In general, a more complex distributed RC model should be considered for diffused integrated circuits when the amplifier is operated over a wide frequency range.¹⁰

A complete equivalent circuit model of the differential amplifier is shown in Fig. B-4. The emitter-bias circuit, including transistor Q_3 , associated resistors and supply voltage V_{EE} , has been replaced by a constant current generator, I_E . Collector-substrate and resistor-substrate capacitances, C_{CS} and C_{RS} , are combined in parallel across the amplifier output resistors, R_{L1} and R_{L2} . The input a. c. signal, e_{1N} , is applied between the base terminals. Radiation effects are accommodated in the model by permanent changes in τ_1 and τ_2 , and transient currents, produced by ionizing radiation, control current generators i_{g1} and i_{g2} .

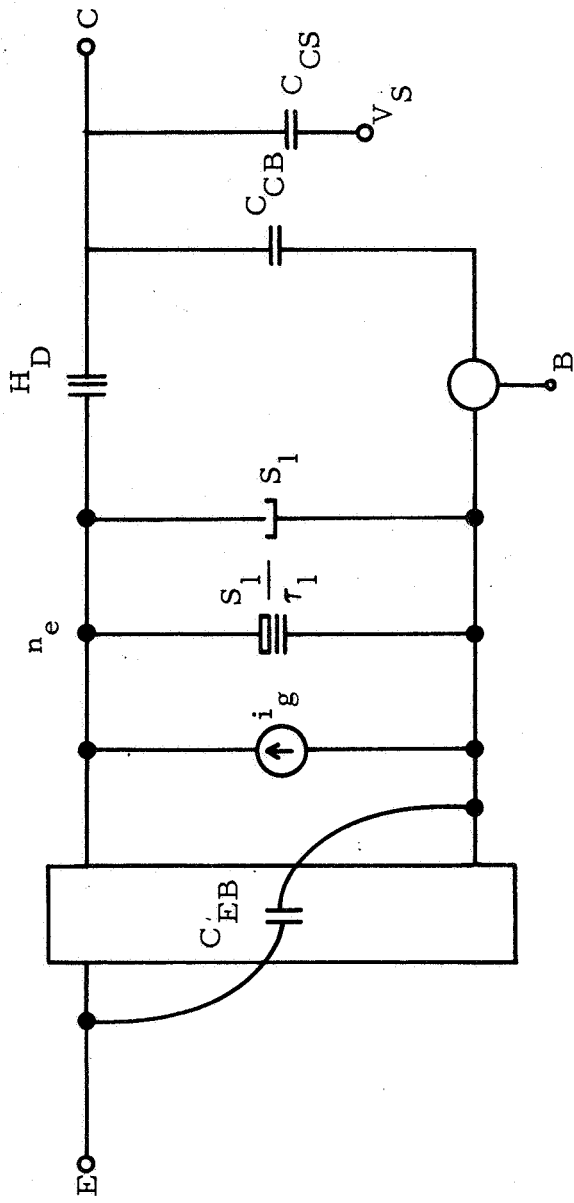


FIG. B-2 APPROXIMATE RADIATION EQUIVALENT CIRCUIT OF INTEGRATED CIRCUIT TRANSISTOR

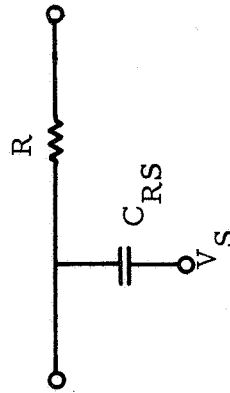


FIG. B-3 APPROXIMATE MODEL OF DIFFUSED RESISTOR

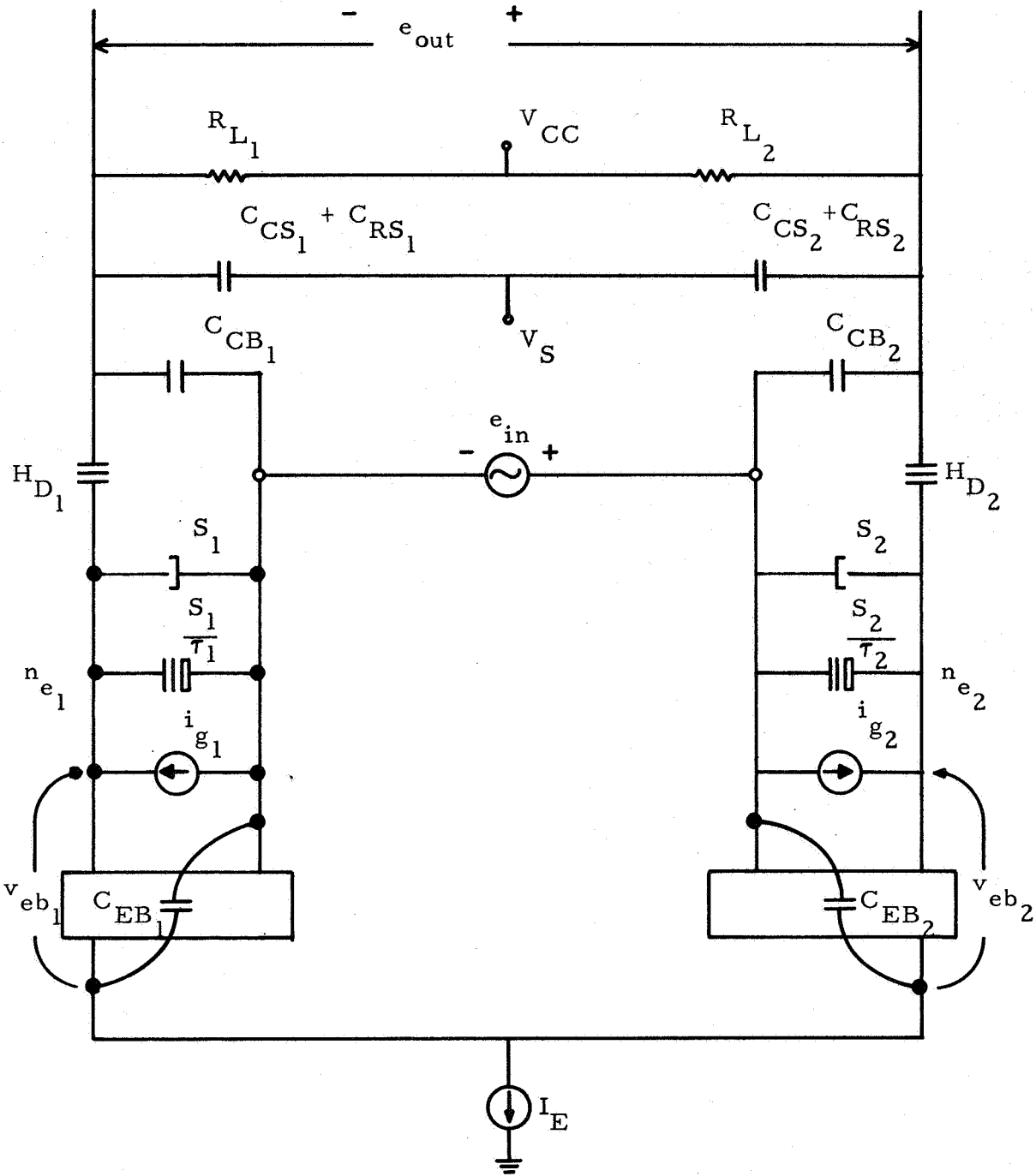


FIG. B-4 COMPLETE EQUIVALENT CIRCUIT MODEL OF DIFFERENTIAL AMPLIFIER

The coded equivalent circuit of Fig. B-5 is used to write an input table for the NASAP computer program. Each element is coded as either a voltage or current source designated by the symbols shown in Fig. B-5. Elements are numbered consecutively starting at the input voltage source (element 1) and ending at element 20 which represents the output voltage measured across a very large resistance (10 megohms) added to the circuit but not affecting its operation. Elements 4 and 5 represent v_{eb} and v_{eb2} , each equal to half the input voltage and opposite in phase as indicated by voltage generators 4 and 5 in Fig. B-5. Transient response current generators i_{g1} and i_{g2} are represented as current source elements 2 and 3. All other elements are represented as either voltage or current sources depending on their location in the circuit topology. All nodes are numbered consecutively starting at the common-emitter junction (bias current generator I_E is omitted in the a. c. model) and ending at node 10 which represents the common bias voltage supply point for V_{cc} and V_S .

An input table describing the coded equivalent circuit to the computer is listed in Table B-I. This description proceeds according to the following steps:

1. Columns A and B describe the nodes of origin and destination for each element listed in column E.
2. Column C describes the type of source (0 for voltage and 1 for current) controlling the element; the control element is given in column D. Passive elements are self-controlled.
3. Column F lists the frequency dependence (1, 0, -1 for corresponding powers of s).
4. Column G states whether element is a voltage or current source (0 for voltage and 1 for current).

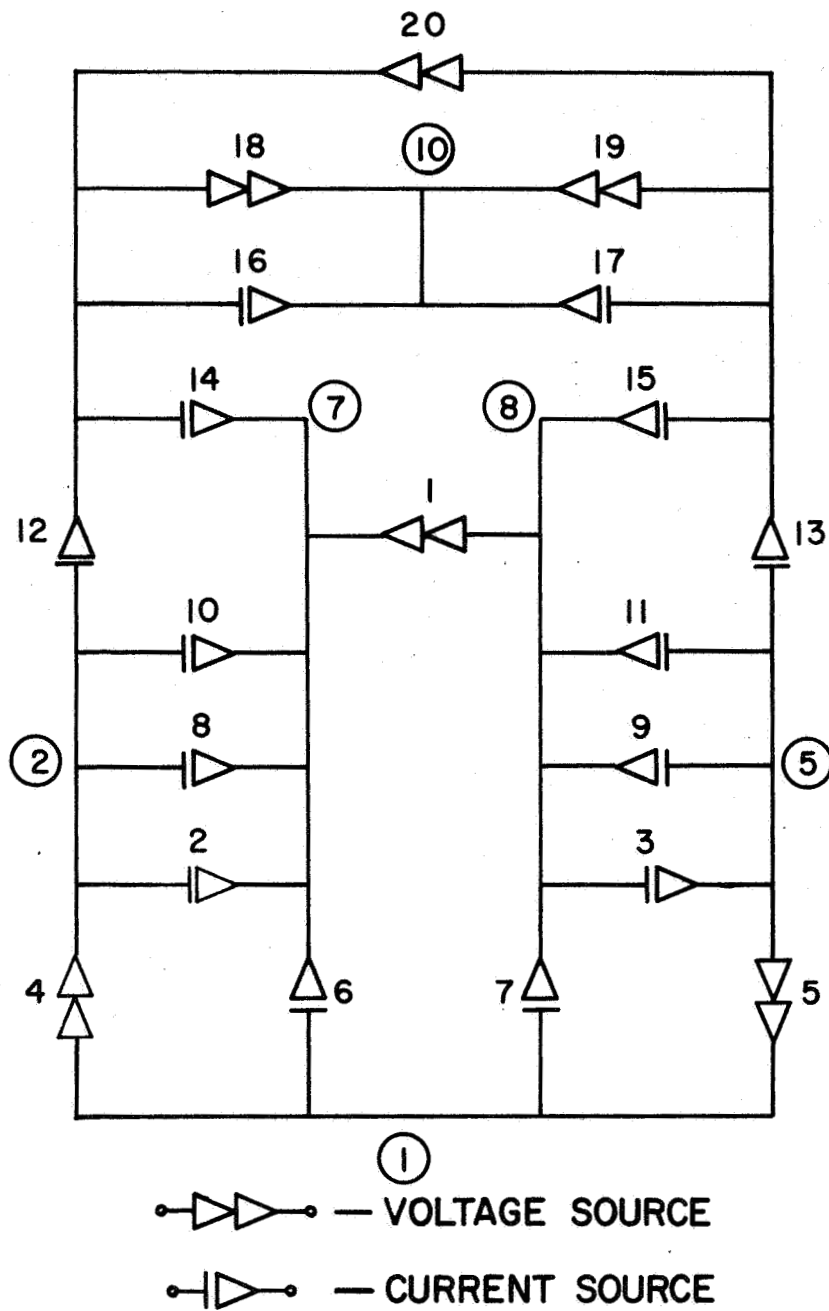


FIG. B-5 CODED EQUIVALENT CIRCUIT

A	B	C	D	E	F	G	H	Numerical
8	7	0	20	1	0	0	1	.100E + 1
3	2	1	2	2	0	1	0	$\frac{\Delta i_g}{2i_g}$
4	5	1	3	3	0	1	0	
2	1	0	1	4	0	0	0	.050E + 1
5	1	0	1	5	0	0	0	
1	3	0	6	6	1	1	0	.710E - 12
1	4	0	7	7	1	1	0	
2	3	0	4	8	0	1	0	$\frac{.310E - 8}{\tau}$
5	4	0	5	9	0	1	0	
2	3	0	4	10	1	1	0	.310E - 8
5	4	0	5	11	1	1	0	
2	6	0	4	12	0	1	0	.217E - 3
5	9	0	5	13	0	1	0	
6	7	0	14	14	1	1	0	.530E - 12
9	8	0	15	15	1	1	0	
6	10	0	16	16	1	1	0	.281E - 11
9	10	0	17	17	1	1	0	
6	10	1	18	18	0	0	0	.840E + 4
9	10	1	18	19	0	0	0	
9	6	20	20	20	0	0	0	.100E + 8

TABLE B-I - Computer Input Table

5. Column H lists the element which represents the input generator which is in turn controlled by the output element to close the system flowgraph.
6. Numerical values of elements are listed according to whether the element is an impedance (current-controlled voltage source), an admittance (voltage-controlled current source), or a controlled or independent (self-controlled) voltage or current source. Linvill elements s , H_c and H_d are entered by first multiply by $\frac{q}{kT} N_E$, according to Eq. (B-7) to obtain an equivalent element which is dependent on voltage v_{eb} . For moderately doped semiconductor material at room temperature, this multiplication constant is approximately $40 \times 10^{18} \text{ volt}^{-1} \text{ cm}^{-3}$.

The input levels of neutron radiation are assumed to vary from 10^{12} to 10^{15} pvt. These values of neutron fluence are entered into the input table through the numerical value of elements 8 and 9 by adjusting the values of τ_1 and τ_2 according to Eq. (6) using $K = 3.5 \times 10^5$ pvt-sec. for the base P-material. The initial value of lifetime, τ_0 , is 10^{-8} seconds for P-type silicon material.

In order to determine the effects of unbalanced ionization between the two halves of the integrated amplifier configuration, an unbalance of Δi_g is assumed between the two radiation current generators i_{g1} and i_{g2} . This unbalance is entered in Table B-I as two current generators opposite in polarity in Fig. B-5 and each with an amplitude $\frac{\Delta i_g}{2i_g}$. This fraction, representing impulse generators, is entered in rows 2 and 3 of the column marked "Numerical" in Table B-I.

The resulting radiation responses of the circuit are illustrated by the curves of Figs. B-6 and B-7. Permanent degradation of differential amplifier gain produced by particle fluence, Φ , from 10^{12} to 10^{15} pvt is shown in Fig. 11. The balanced configuration helps to maintain amplifier gain at reasonable levels

(above 30), even though a sizeable radiation field has been encountered. The peak amplitude transient response due to ionization radiation demonstrates considerable suppression resulting from common mode rejection of the differential amplifier stage. Corresponding responses from unbalanced configurations are an order of magnitude larger in peak amplitude.⁴

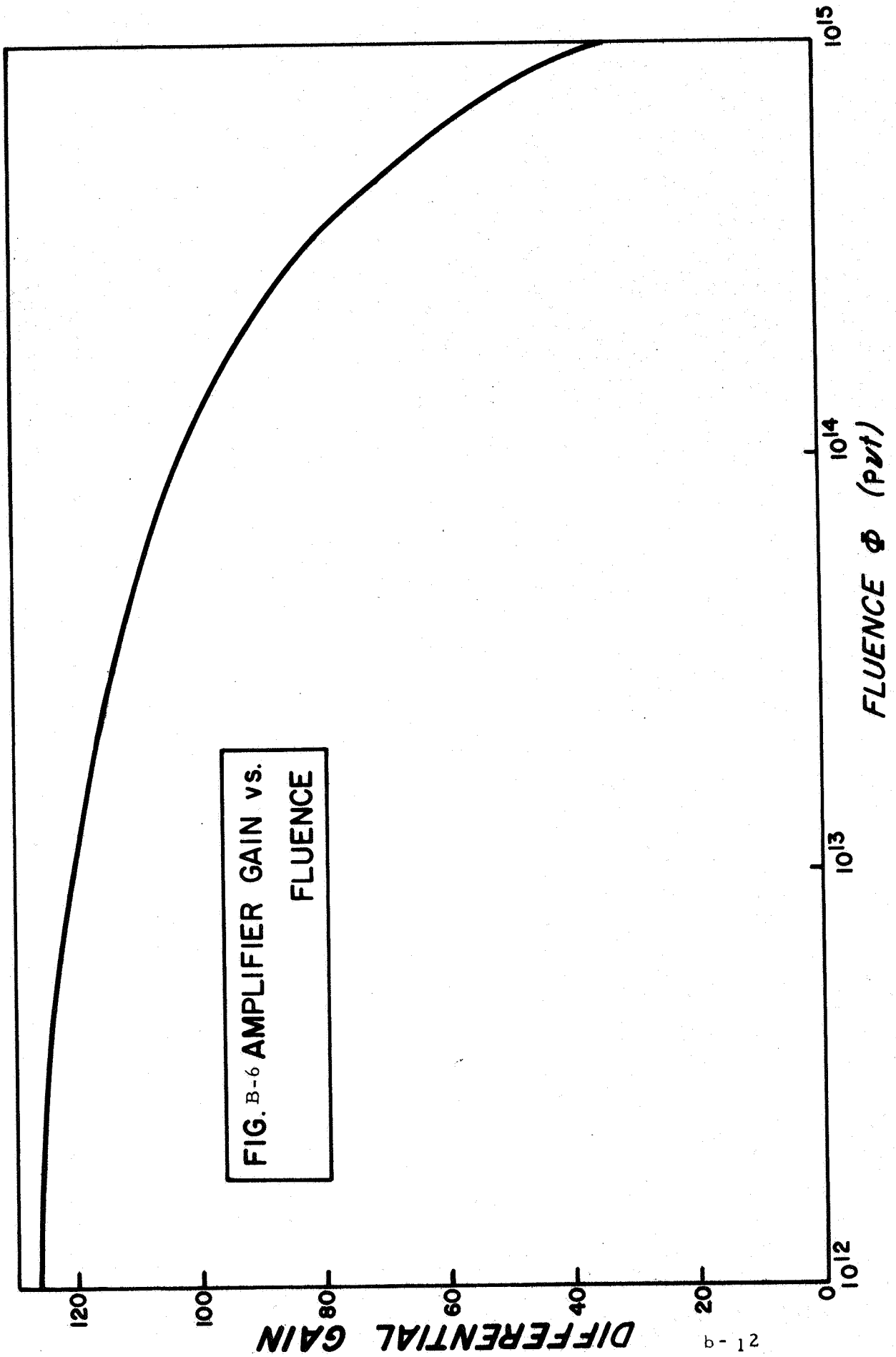


FIG. B-6 AMPLIFIER GAIN vs.
FLUENCE

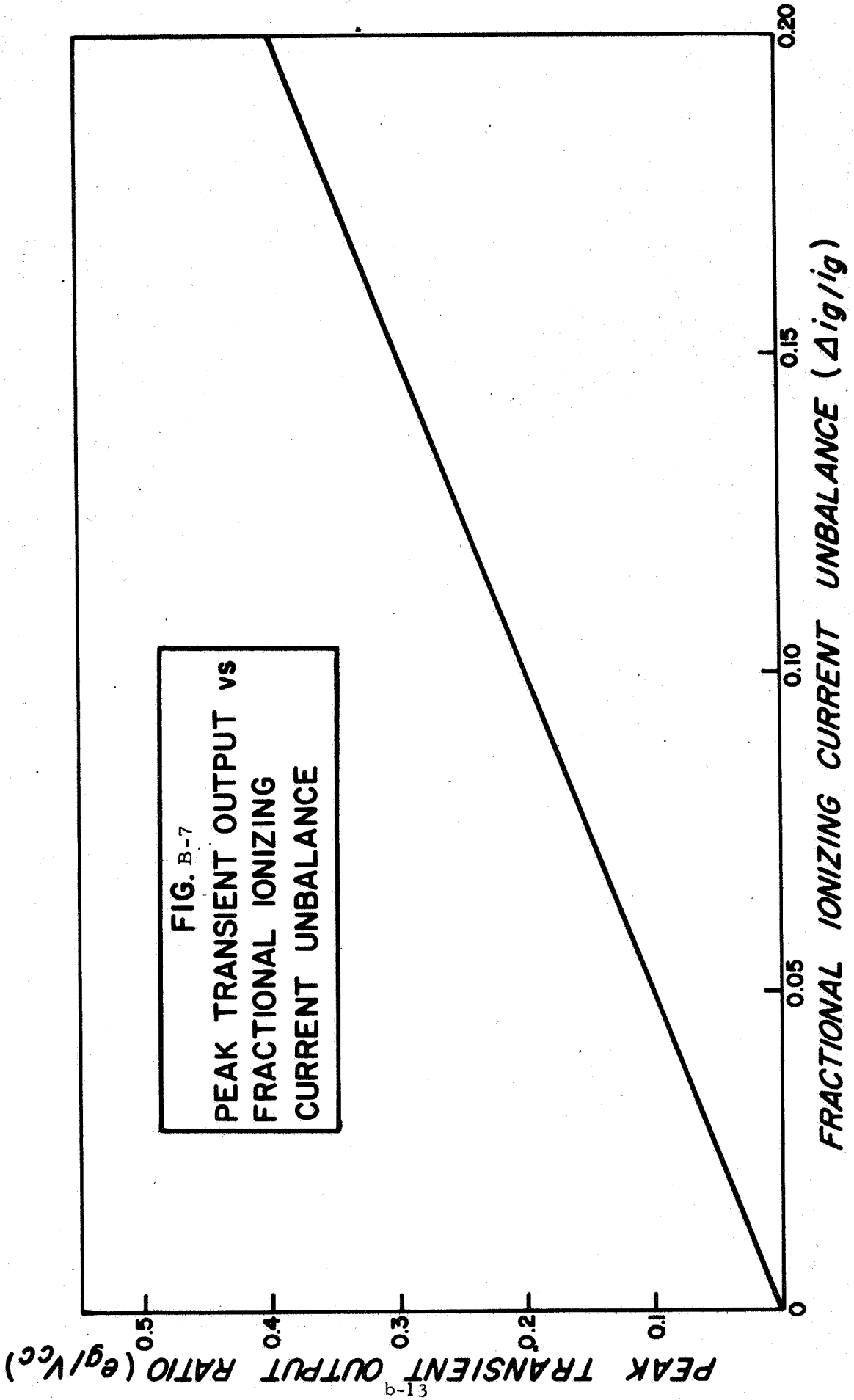


FIG. B-7
PEAK TRANSIENT OUTPUT vs
FRACTIONAL IONIZING
CURRENT UNBALANCE

APPENDIX C: AUTOMATED DESIGN OF NETWORKS WITHIN SPECIFIED RESPONSE AND IMPEDANCE CONSTRAINTS

One of the major design considerations in selecting the components of a network is the maintenance of network responses and impedance levels within the constraints imposed by system requirements. This is especially critical in the design of microcircuits, where the component values and tolerances limited by the technology used to realize the circuit. The size, cost, and reliability of an integrated circuit is determined primarily by the component values and tolerances allowed in the design.²⁴

The theory needed to develop the design algorithms to achieve these objectives is available in the network literature.^{32, 33} The basis for the procedure to be developed here is a congruence transformation suggested by Cauer in 1929 which allows one physically realizable network to be generated from another in such a way that specified driving point and/or transfer functions are held invariant.³² Networks with different numbers of elements and nodes, having the same driving point and/or transfer functions, may be generated by use of this transformation. Although Cauer first suggested this technique for passive networks, its strength is enhanced when applied to active networks, as will be illustrated in this paper. Application of this theory to the development of a continuously equivalent network theory for the synthesis of minimum sensitivity networks was suggested by Schoeffler.³⁴ By generating networks whose elements differ from those of the original network by an incremental amount, he developed differential equations for both the change in element values and the sensitivities of the transfer function and/or impedances, thus allowing realization of minimal sensitive networks.

Although the concept of continuously equivalent network theory is clearly presented in reference 34, the pertinent results will be reviewed here for completeness. Consider a network with \underline{n} independent node pairs described by a set of \underline{n} equations of the form

$$I = Y_0 E \quad (C-1)$$

where Y_0 is the $\underline{n} \times \underline{n}$ admittance matrix of the network, E is the $\underline{n} \times 1$ column matrix of node voltages, and I is the $\underline{n} \times 1$ column matrix of source currents.

There exists an infinite number of equivalent networks (at specified terminals) with network variables related by

$$I' = Y' E' \quad (C-2)$$

where

$$I' = A^t I \quad (C-3)$$

$$E = A E' \quad (C-4)$$

$$Y' = A^t Y_0 A \quad (C-5)$$

and A is an $\underline{n} \times \underline{n}$ nonsingular constant matrix, t denotes the transpose, and I' , E' , and Y' are the new current and voltage variables and admittance matrices of the equivalent network. By proper choice of the transformation matrix A , certain driving point and/or transfer functions can be held invariant. For example, if the k^{th} row of A is the k^{th} unit vector (all zeros except for the k^{th} entry which is unity), the driving point impedance at the k^{th} terminal pair is invariant to the transformation. If two rows are so chosen, the driving point impedance at each port is invariant as is the transfer impedance between the two ports.

Schoeffler suggested that the A matrix produce an incremental change from the original network to the equivalent one by letting

$$A = U + B \Delta x \quad (C-6)$$

where

$$b_{ij} \leq 1$$

U = unit matrix

x is an independent variable

Substituting (C-5) and (C-6), considering the admittances of the new network a continuous function of x, and taking the limit as $\Delta x \rightarrow 0$ results in the following differential matrix equation.

$$\frac{dY}{dx} = B^t Y + YB \quad (C-7)$$

with initial conditions

$$Y(0) = Y_0 \quad (C-8)$$

For any choice of B, the solution to this set of differential equations at any value of x gives a realizable admittance matrix. In order to maintain a transfer function invariant, any row of A which is a unit vector implies that the same row of B must be identically zero. For elements of the network which are to remain passive, the transformation must result in an entry at the associated admittance matrix which is positive or zero. This is accomplished by choosing the unspecified elements of B in such a way that the final value of admittances in Y is positive or zero for passive elements.

A more convenient form for the first-order matrix differential equation given by (C-7) which separates out the various types of elements of the network is

$$\frac{dE_i}{dx} = ME_i \quad (C-9)$$

where E_1 is an $n \times n$ matrix of all of one type of element connected to the nodes of the network, e.g., capacitors, inductors, conductances, and controlled sources. The constant matrix M is identical for all of the elements regardless of frequency dependence or passivity. This is illustrated by the following RC network example.

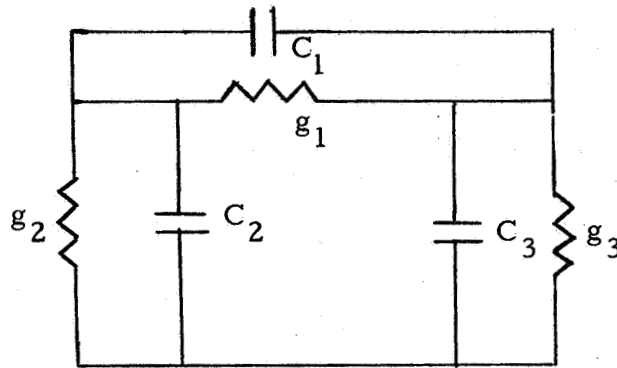


Fig. C-1 Example of RC Network

$$Y = \begin{bmatrix} g_1 + g_2 & -g_1 \\ -g_1 & g_1 + g_3 \end{bmatrix} + s = \begin{bmatrix} C_1 + C_2 & -C_1 \\ -C_1 & C_1 + C_3 \end{bmatrix} \quad (C-10)$$

and

$$B = \begin{bmatrix} b_1 & b_2 \\ b_3 & b_4 \end{bmatrix} \quad (C-11)$$

Substituting (C-10) and (C-11) into (C-7) results in the two first-order differential matrix equations

$$\frac{dG}{dx} = MG \quad (C-12)$$

and

$$\frac{dC}{dx} = MC \quad (C-13)$$

where

$$G = \begin{bmatrix} g_1 \\ g_2 \\ g_3 \end{bmatrix} \quad C = \begin{bmatrix} C_1 \\ C_2 \\ C_3 \end{bmatrix} \quad (C-14)$$

$$M = \begin{bmatrix} b_1 + b_4 - b_2 - b_3 & -b_2 & -b_3 \\ b_1 - b_4 + b_2 - b_3 & 2b_1 + b_2 & b_3 \\ b_3 + b_4 - b_1 - b_2 & b_2 & 2b_4 + b_3 \end{bmatrix} \quad (C-15)$$

In general, the differential equations for the elements of the network will be in the form of (C-9) where the matrix M has elements which are linear combinations of the b_i and are arbitrary. Some of the b_i will be zero by the requirement of invariance of a transfer function and/or impedance of the network. The remaining b_i are free to satisfy the tolerance design requirements.

The procedure for the design of networks within specified response and impedance constraints is based upon a formulation of the sensitivity function $S_{e_k}^F$ given by Eq. (26) in terms of the theory of continuously equivalent networks,³⁴ The results of the derivation of network function sensitivity to changes in the individual elements are:

$$\frac{dQ_{e_k}}{dx} = -M^t Q_{e_k} \quad (C-16)$$

where

$$Q_{e_k} = \begin{bmatrix} q_{e_1} \\ \vdots \\ q_{e_n} \end{bmatrix} \quad \text{and} \quad q_{e_k} = \frac{S_{e_k}^F}{e_k}$$

and the matrix M^t is the transpose of the matrix M relating the change in element matrix E_1 with respect to independent variable x to the original E_1 matrix. Thus, once the differential matrix equation for the changes in elements has been determined, the differential matrix equation for the change in element sensitivities is also determined.

The next step in the development of a design procedure is to examine the

statistical tolerance, Equation (25). Note that for a given set of component tolerance $\frac{de_k}{e_k}$, the network function tolerance is calculated from Eq. (27).

If this network function tolerance is not within the system constraint limit, the network elements must be changed to lower the sensitivity functions weighted by the component tolerances. This must be done within the limits of available component values, and the passive elements must remain positive or zero.

Squaring both sides of Eq. 25 and the terms inside and recognizing that $\frac{de_k}{e_k}$ is real,

$$S = \left(\frac{\Delta F_S}{F} \right)^2 = \sum_{k=1}^n \left| S_{e_k}^F \right|^2 \left(\frac{de_k}{e_k} \right)^2 \quad (C-17)$$

This summation may be expressed in terms of the q_{e_k} elements defined below equation (C-15):

$$S = \sum_{k=1}^n \left| q_{e_k} \right|^2 (de_k)^2 = \sum_{k=1}^n q_{e_k} q_{e_k}^* (de_k)^2 \quad (C-18)$$

For a given network function, the statistical tolerance ΔT_S is lowered when the summation S is lowered. Differentiating S to determine the slope as a function of increasing x,

$$\frac{dS}{dx} = 2 \sum_{k=1}^n \operatorname{Re} \left(\frac{dq_{e_k}}{dx} q_{e_k}^* \right) (de_k)^2 \quad (C-19)$$

This derivative may be written in matrix notation:

$$\frac{dS}{dx} = -2Q_{e_k}^t \left[D_{de_k}^2 M^t + MD_{de_k}^2 \right] Q_{e_k} \quad (C-20)$$

where the Q_{e_k} and E matrices are column matrices, and the D_{e_k} matrices are diagonal matrices defined by

$$D_{e_k} = \text{Diag} [e_1, e_2, e_3, \dots, e_k, \dots, e_n]$$

The fact that M is real is used to derive Eq. (C-20).

Equation (C-20) is the key to a design procedure. The element of diagonal matrix D is determined by the technology used in realizing the network elements as well as cost, size, and reliability considerations. The elements of the Q matrices are computed for the original network using the NASAP program. The b_i elements of the M matrix are available for increasing the negative slope of S according to Eq. (C-20). This is done by taking the b_i 's plus or minus one, depending upon the sign of its coefficient in (C-20). Once the M matrix, whose elements are a linear combination of the free parameters of the transformation in (C-7), has been determined, the new elements are calculated by solving the differential equations given by (C-9). This procedure is repeated until the required statistical tolerance limits have been met. Each time a new set of b_i elements is chosen however, care must be taken not to allow any of the passive elements to go negative or beyond the limits of the component values allowed by the realization technology.

The computer calculations required by this design procedure are:

1. Calculation of Q_e matrix
2. Integration of differential equations given by C-9.

The first calculation is performed using the available tagging options in the NASAP program from the preceding network. The second calculation requires integration of a set of linear differential equations with constant coefficients, since M is assumed constant for each integration. This is easily performed on the digital computer. Therefore, by writing a simple auxiliary program, NASAP may be adapted to implement this very powerful automated design procedure.

APPENDIX D: MICROCIRCUIT FILTER DESIGN WITH COMPUTER
ORIENTED OPTIMIZATION**

Ezra Zeheb*
Visiting Assistant Professor of Electrical Engineering
Stevens Institute of Technology
Hoboken, New Jersey

Active RC synthesis techniques are now well known.³⁵ Most of the networks resulting from these design procedures are suitable, in a sense, for integrated circuit fabrication because they are inductorless and because fabrication techniques for resistors, capacitors and most of the basic active elements are well established.²⁴ However, since these methods are not particularly directed towards integrated circuit fabrication, they suffer from many disadvantages when used as such, in particular from the economical point of view.

A method which overcomes this has been proposed by Newcomb et. al.³⁶ The components utilized are capacitors and gyrators and the network is resistance terminated. All gyrators are grounded and, thus, the network is perfectly suitable for integrated circuit fabrication. Also, the number of capacitors utilized is minimum.

Though very practical from the viewpoint of production, the method has a disadvantage from the viewpoint of design, since it introduces a new type of section. In this paper we show that identical results can be arrived at by simple and known derivations. Also, the intermediate stage in the derivation

* On leave of absence from Technion-Israel Institute of Technology, Haifa, Israel.

** This Appendix was presented as a paper at the 11th Midwest Symposium on Circuit Theory, University of Notre Dame, Indiana; May, 1968.

allows for a configuration most convenient for automatic analysis by NASAP.

An optimal parameter can be determined for minimum multi-parameter sensitivity, for example.

As in reference 36, the function which is considered is a rational positive real (PR) input admittance. This is no loss in generality, since it is well known that given, for example, a transfer voltage ratio magnitude $V_2(j\omega)/V_s(j\omega)$ ² under given resistive load and source terminations, (Fig. D-1), one can compute the input admittance $y(j\omega)$ by

$$\left| \frac{y(j\omega) - G_1}{y(j\omega) + G_1} \right|^2 = 1 - 4 \frac{G_2}{G_1} \left| \frac{V_2(j\omega)}{V_s(j\omega)} \right|^2 \quad (D-1)$$

This relation assumes

$$1 \geq 4 \frac{G_2}{G_1} \left| \frac{V_2}{V_s} \right|^2 \quad (D-2)$$

but if this is not the case, a constant gain amplifier can always be inserted at the output.

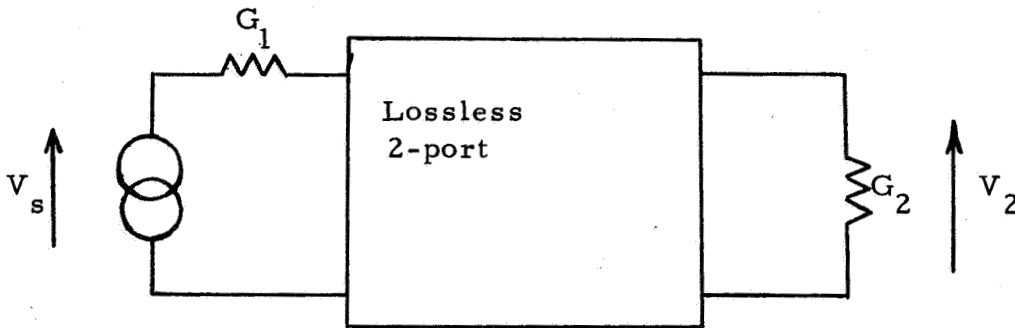
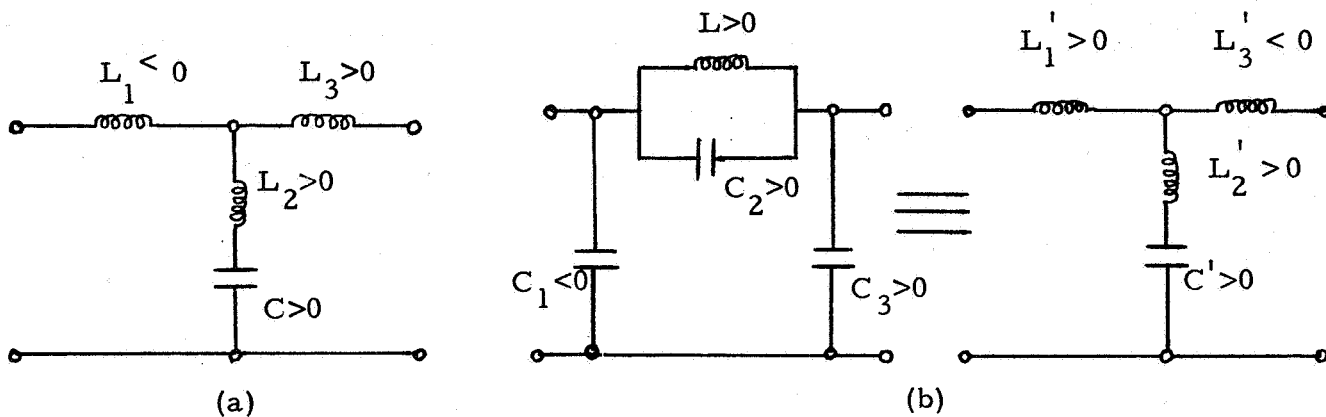


Fig. D-1

The interesting case for filters is, of course, where the zeros of transmission, which are the zeros of the even part of $y(s)$, are purely imaginary. Brune's³⁷ section for realizing a pair of conjugate imaginary zeros is very well known where the first element is a series negative inductor or a shunt negative

capacitor which results in a series positive inductor (See Fig. D-2). Less common and less known, though not different in principle, are the equivalent Brune's sections where the first element is a series negative capacitor (which results in a shunt positive inductor) or a shunt negative inductor (Fig. D-3). The pertinent expressions are derived for the sake of completeness.



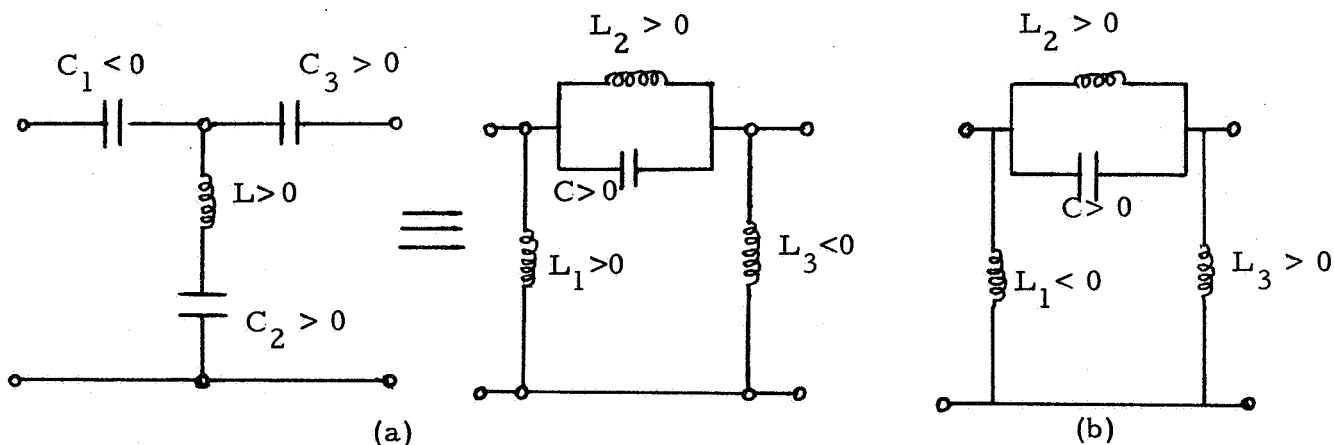
$$\omega_0^2 = \frac{1}{L_2 C}$$

$$L_1 L_2 + L_1 L_3 + L_2 L_3 = 0$$

$$\omega_0^2 = \frac{1}{L_2' C'}$$

$$L_1' L_2' + L_1' L_3' + L_2' L_3' = 0$$

Fig. D-2



Given a driving point admittance $y(s)$, the even part of which has zeros at $\pm s = j\omega_0$, we have

$$y(j\omega_0) = jB \quad (D-3)$$

where B is a real number.

Removing a shunt inductor L_1 to produce an imaginary zero, we have

$$y_1(s) = y(s) - \frac{1}{sL_1} \quad (D-4)$$

where

$$L_1 = -\frac{1}{\omega_0 B} = \frac{1}{j\omega_0 \cdot y(j\omega_0)} \quad (D-5)$$

We then remove from $Z_1(s) = \frac{1}{y_1(s)}$ a resonant circuit to receive

$$Z_2(s) = Z_1(s) - \frac{s/c}{s^2 + \frac{1}{L_2 c}} = \frac{1}{y(s) - \frac{1}{sL_1}} - \frac{s/c}{s^2 + \frac{1}{L_2 c}} \quad (D-6)$$

where

$$L_2 = \frac{1}{\omega_0^2 c} \quad (D-7)$$

and $\frac{1}{c}$ is twice the residue of $Z_1(s)$ in its pole at $s = j\omega_0$, namely,

$$\frac{1}{c} = 2 \left[\frac{d}{ds} \frac{1}{Z_1} \right]_{s=j\omega_0}^{-1} = 2 \left[\frac{dy}{ds} + \frac{1}{s^2 L_1} \right]_{s=j\omega_0}^{-1} \quad (D-8)$$

or

$$c = \frac{1}{2} \left[\frac{dy}{ds} \Big|_{s=j\omega_0} - \frac{1}{\omega_0^2 L_1} \right] \quad (D-9)$$

Now let $y(s) = \frac{P}{Q}$. Then

$$Z_2(s) = \frac{Q s L_1}{P s L_1 - Q} - \frac{s L_2}{1 + \frac{s^2}{\omega_0^2}} \quad (D-10)$$

where $PsL_1 - Q$ has $1 + \frac{s^2}{\omega_0^2}$ as a factor.

Therefore,

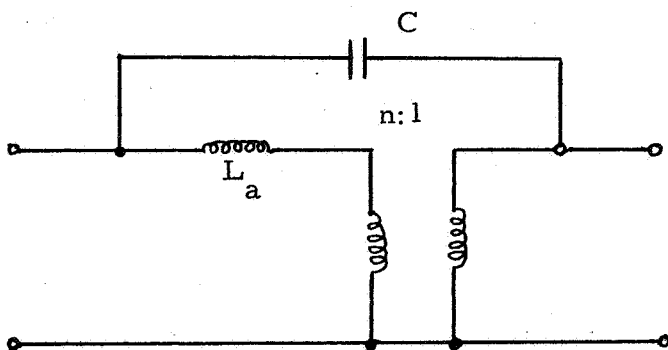
$$Z_2(s) = \frac{s \left[QL_1 - L_2 \left(\frac{PsL_1 - Q}{1 + s^2/\omega_0^2} \right) \right]}{PsL_1 - Q} \quad (D-11)$$

vanishes at the origin, and $y_2(s) = \frac{1}{Z_2(s)}$ has a pole at the origin with residue $-\frac{1}{L_1 + L_2}$. Therefore, removing a shunt inductor

$$L_3 = -(L_1 + L_2) \quad (D-12)$$

yields a remainder positive real function two degrees less than the original $y(s)$.

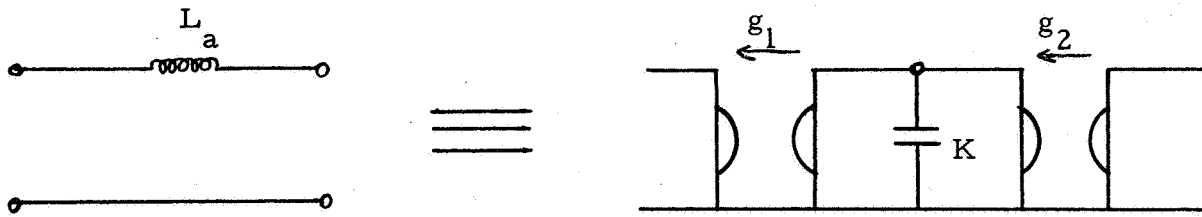
Using the equivalent representation (Fig. D-4) and then replacing the inductor by a grounded gyrator³⁸ (Fig. D-5), we arrive at the network shown in Fig. D-6 where K is arbitrary and



$$L_a = \frac{L_1 L_2}{L_1 + L_2}$$

$$n = \frac{L_1}{L_1 + L_2}$$

Fig. D-4



$$L_a = K/g_1^2$$

Fig. D-5

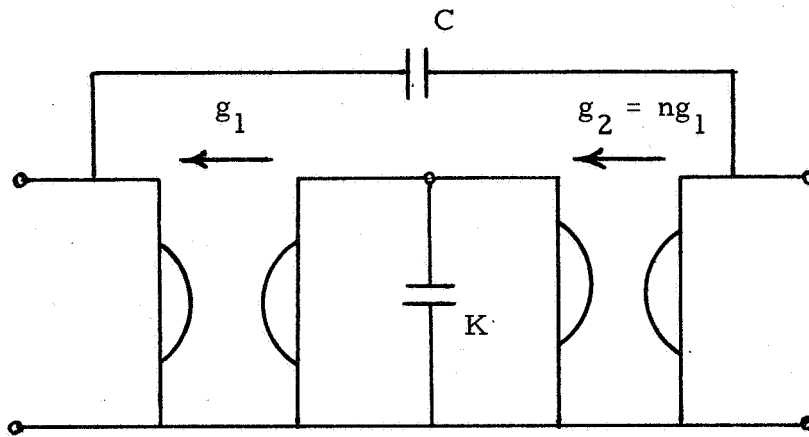


Fig. D-6

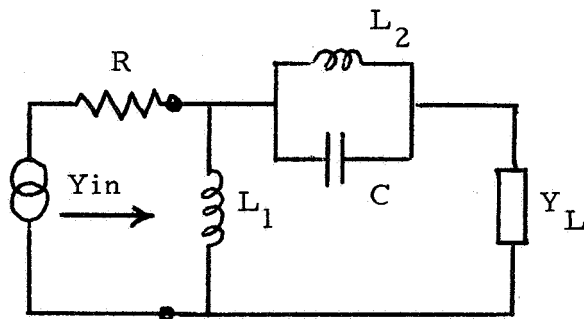


Fig. D-7

$$g_1^2 = \frac{K}{L_a} = \frac{L_1 + L_2}{L_1 L_2} \quad K = K\omega_0^2 \frac{y'(j\omega_0) - \frac{y(j\omega_0)}{j\omega_0}}{2} \quad (D-13)$$

$$g_2 = ng_1 = \frac{L_1}{L_1 + L_2} \quad g_1 = g_1 \frac{y'(j\omega_0) + \frac{y(j\omega_0)}{j\omega_0}}{y'(j\omega_0) - \frac{y(j\omega_0)}{j\omega_0}} \quad (D-14)$$

$$c = \frac{1}{2} \left[y'(j\omega_0) + \frac{y(j\omega_0)}{j\omega_0} \right] \quad (D-15)$$

The section described in Fig. D-6 and Eqs. (D-13) to (D-15) is identical to the pertinent one in reference 36. However, one does not have to apply and adopt new types of sections. One can just use the well-established Brune's philosophy to carry on all design considerations and calculations on this network, and then simply replace all inductors by capacitors and grounded gyrators. Incidentally, if the degree of the function to be realized is high, then in most practical cases one can realize two functions of half the degree plus or minus one by applying the theorems and method described by Navot and Zeheb.^{39, 40}

The section in Fig. D-6 has an arbitrary parameter K free to be chosen so that the network is optimized in some respect. Using the statistical tolerance ΔT_S in the form

$$T_y = \sqrt{\sum_{i=1}^n \left(\frac{\partial y}{\partial X_i} X_i \right)^2} \quad (D-16)$$

where y is a network function and X_i ($i = 1, 2, \dots, n$) are the network elements, yields

$$y = f(X_1, X_2, \dots, X_n) \quad (D-17)$$

This task fits excellently to NASAP, except that the configuration described in Fig. D-6 is not convenient. However, before the replacement is carried out, the configuration is most suitable. Therefore, expressing the element values in terms of K , c , g_1 , and g_2 , namely

$$L_1 = \frac{L_a}{1-n} = \frac{K}{g_1(g_1 - g_2)} \quad (D-18)$$

$$L_2 = \frac{L_a}{n} = \frac{K}{g_1 g_2} \quad (D-19)$$

$$L_3 = -(L_1 + L_2) = -\frac{K}{g_2(g_1 - g_2)} \quad (D-20)$$

makes it possible to solve for an optimal K which minimizes, for instance,

T_y or $T_{y/y}$.

Of particular interest is to minimize the multiparameter sensitivity at the function's transmission zeros frequencies, and thus keep them close to their desired locations and keep the behaviour of the function in their vicinity, as close as possible to the desired. As shown in the sequel, if one can assume that variations in elements values are not too large, the optimal parameter C_x for the sensitivity of the function in these frequencies can be determined and written in close form for all given numerical functions.

Denote by Y_L the admittance of the part of the network which is to the right of the first anti-resonance circuit Fig. D-7. If the value of the product $L_2 C$ is sufficiently close to the desired one, then, at the transmission zero frequency $\omega_0 = \sqrt{\frac{1}{L_2 C}}$ the anti-resonance circuit can be considered as an

open-circuit. Therefore, the influence of Y_L on the behaviour of the function at that frequency may be neglected. It remains to minimize the sensitivity of L_1 to variations in g_1 , g_2 and C_x .

To be specific, assume the gyration ratios g_1 and g_2 are directly proportional to resistors in the network which are of the doped semiconductor type, that the integrated capacitors are of the junction type, and consider the sensitivity to temperature variations.

The effects of temperature on these integrated elements can be approximated as follows for an abrupt junction:

$$\frac{dg_i}{dT} = nT^{n-1} \quad (i = 1, 2) \quad (D-21)$$

$$C = \sqrt{\frac{q\epsilon N_a N_d}{2(N_a + N_d)}} \frac{1}{\sqrt{V_d + V_R}} \quad (D-22)$$

$$V_d = -\frac{3k}{q} T \ln T - \frac{0.28 \times 10^{-3}}{q} T \quad (D-23)$$

where T is the absolute temperature, n is a constant which depends on the doping level (can be assumed to equal 1.5 for moderate doping), q is the charge of an electron, ϵ is the dielectric constant, N_a and N_d are the densities of the acceptor and donor impurities, V_R is the reverse applied voltage, V_d is the contact potential and k is Boltzmann's constant.

Using Eqs. (D-13), (D-14), (D-21), (D-22) and (D-23) one can easily compute

$$\left. \frac{dL_1}{dT} \right|_{T=T_0} = \left[\frac{\partial L_1}{\partial g_1} \frac{dg_1}{dT} + \frac{\partial L_1}{\partial g_2} \frac{dg_2}{dT} + \frac{\partial L_1}{\partial C_x} \frac{dC_x}{dT} \right]_{T=T_0} = \frac{\mu}{\sqrt{C_x}} + \frac{\eta}{C_x} \quad (D-24)$$

where,

$$\mu = \frac{n T_0^{n-1}}{a^2 (b - a)}$$

$$\eta = \frac{1}{a(a-b)} \sqrt{\frac{\epsilon N_a N_d}{8q(N_a + N_d)}} (V_{d0} + V_R)^{-3/2} \left[3k(1 + \ln T_0) + 0.28 \times 10^{-3} \right]$$

$$V_{d0} = V_d \quad T = T_0$$

For zero sensitivity at a prescribed temperature T_0 , one has to choose either very large values for the capacitor C_x , or, since η and μ are of different signs,

$$C_x = \frac{\eta^2}{\mu^2} \tag{D-25}$$

The first choice might be impractical from the viewpoint of production.

The choice of C_x through Eq. (30) is done independently for every section of the filter, using its own coefficients a and b or μ and η .

Instead of minimizing the sensitivity of L_1 , one might wish to minimize that of the product $L_2 C$. A similar Eq. to (D-24) is arrived at, only the constants μ and η are different. If the constants are such that practical values of C_x are large enough to render sufficiently low sensitivities, both L_1 and $L_2 C$ can become insensitive.

APPENDIX E: SENSITIVITY AND WORST CASE COMPUTATIONS FOR
NONLINEAR SYSTEMS

The concept of sensitivity is used to determine the effect of parameter variation on circuit behavior. In linear systems, the parameter is one of the element coefficients such as β , R, etc. For nonlinear systems, the parameter corresponds to one of the factors effecting the function, other than the intended variable. For instance, the quantity I_S of $f_G(v) = I_S(\epsilon^{39v} - 1)$ may be a parameter of variation and v is the intended variable.

Equation (E-1) defines sensitivity as a percentage rate of change.

$$S_P^y = \frac{P}{y} \frac{\partial y}{\partial P} \quad (E-1)$$

where

P is the parameter of variation

y is a measure of circuit behavior (output).

Quite often, S_P^y is determined under steady state d-c conditions. In general, however, the sensitivity is a function of time. If the system is linear, S_P^y is expressible as a function of the LaPlace complex frequency. It is intended here to compute the transient sensitivity in lieu of steady state d-c. Since the systems treated are nonlinear, closed form solutions of sensitivity are beyond the realm of achievement. Therefore, a numerical transient computation of sensitivity will be described. Furthermore, the sensitivity of the user selected outputs ($\underline{Y}(t)$) will be determined.

For small variations of P , one can approximate equation (E-1) as

$$S_P^y \approx \frac{P}{y} \frac{\Delta y}{\Delta P} \quad (E-2)$$

where Δy is the change in y corresponding to the change in P .

The user will be required to specify the change in P . This will be done by indicating two functions for one of the elements when part 2 of the program is performed. For instance, if $f_{\beta 7}(i_4)$ is to vary in the preceding example, the user would specify $f_{\beta 7}(i_4)$ and $f'_{\beta 7}(i_4)$. More than one term of a function is allowed to vary; e. g.,

$$f_{\beta 7}(i_4) = 100 i_4 \epsilon^{-.1 |i_4|}$$

$$f'_{\beta 7}(i_4) = 105 i_4 \epsilon^{-.09 |i_4|}$$

That is, the sensitivity with regard to the variation of an entire function can be computed. It is important to point out that if more than one parameter of a function is to vary, then the second set of parameters should alter the function in the same direction, if possible. For example, $f'_{\beta 7}(i_4) = 105 i_4 \epsilon^{-1.1 |i_4|}$ is less desirable than the preceding equation for $f'_{\beta 7}(i_4)$.

It is also important to point out that if only one term "P" of a function is varied, then the computation of $P/\Delta P$ is superfluous. This is because P and ΔP are known to the user; e. g.,

$$f_G(v) = 10^{-6} (\epsilon^{39v} - 1)$$

$$f'_G(v) = (1.1) (10^{-6}) (\epsilon^{39v} - 1)$$

$$P = 10^{-6}$$

$$\Delta P = 10^{-7}$$

For this reason, P , ΔP , and $P/\Delta P$ will not be computed by the program. A combination of the following outputs will be available:

$\underline{Y}(t)$ (Time responses of user selected outputs.)
 $\underline{\Delta Y}(t)$ (Time responses of output changes.)

$\left. \begin{array}{l} \Delta y_1(t)/y_1(t) \\ \vdots \\ \Delta y_n(t)/y_n(t) \end{array} \right\}$ (Percentage changes of output time responses. Computed only when $|y_j(t)| > \epsilon > 0$.)

$f(x(t))$ (Time response of function with the varying parameter.)

$\Delta f(x(t))$ (Time response of difference of the two functions.)

$f(x(t))/\Delta f(x(t))$ (Inverse percentage change of the function. Computed only when $|\Delta f(x(t))| > \epsilon > 0$.)

$S_f^{y_1} = \frac{\Delta y_1(t)}{y_1(t)} \cdot \frac{f(x(t))}{\Delta f(x(t))}$
 \vdots
 $S_f^{y_n} = \frac{\Delta y_n(t)}{y_n(t)} \cdot \frac{f(x(t))}{\Delta f(x(t))}$ } (Sensitivity with regard to function variation. Computed only when $|y_j(t)|, |\Delta f(x(t))| > \epsilon > 0$.)

The threshold of computation " ϵ " is a variable which depends upon the percentage which has been computed.

The algorithms for computing the above quantities are relatively straightforward. In discussing the algorithms, the vector \underline{P} will represent the original values of the parameters in the function which is to vary. The vector \underline{P}' will represent the second set of parameters. It should be clear that the set of parameters introduces a new set of variables in the equations of chapter 4. All quantities which utilize \underline{P}' will be designated by a prime; e.g., $\underline{v}'_c(t)$. Those quantities which utilize \underline{P} in their evaluation will not be primed. Observe that the independent sources $\underline{v}_g(t)$ and $\underline{i}_g(t)$ are unaffected by the varying parameters.

The following basis will be used in the computations: Assuming a common state ($\underline{q}(t)$, $\underline{\lambda}(t)$), the effect of changing from \underline{P} to \underline{P}' will be computed at time $t + \Delta t$. The reason time $t + \Delta t$ is used, is to allow the parameter changes to affect the state. That is, the state is dependent upon the parameters, and its rate of change with respect to the parameters must be incorporated into the computations.

The order in which computations are made is designated by the series of equations shown below. The order essentially follows the flow chart of Figure 15.

$$\underline{v}_c(t) = \underline{f}_S [\underline{q}(t), \underline{P}]$$

$$\underline{v}'_c(t) = \underline{f}_S [\underline{q}(t), \underline{P}']$$

$$\underline{i}_L(t) = \underline{f}_I [\underline{\lambda}(t), \underline{P}]$$

$$\underline{i}'_L(t) = \underline{f}_I [\underline{\lambda}(t), \underline{P}']$$

$$\underline{i}_c(t) = \underline{G}_c \left[\begin{array}{l} \underline{v}_g(t), \underline{i}_g(t), \\ \underline{v}_c(t), \underline{i}_L(t), \underline{P} \end{array} \right]$$

$$\underline{i}'_c(t) = \underline{G}_c \left[\begin{array}{l} \underline{v}_g(t), \underline{i}_g(t), \\ \underline{v}'_c(t), \underline{i}'_L(t), \underline{P}' \end{array} \right]$$

$$\underline{v}_L(t) = \underline{G}_L \left[\begin{array}{l} \underline{v}_g(t), \underline{i}_g(t), \\ \underline{v}_c(t), \underline{i}_L(t), \underline{P} \end{array} \right]$$

$$\underline{v}'_L(t) = \underline{G}_L \left[\begin{array}{l} \underline{v}_g(t), \underline{i}_g(t), \\ \underline{v}'_c(t), \underline{i}'_L(t), \underline{P}' \end{array} \right]$$

$$\underline{q}(t+\Delta t) = \underline{q}(t) + \int_t^{t+\Delta t} \underline{i}_c(\tau) d\tau$$

$$\underline{q}'(t+\Delta t) = \underline{q}(t) + \int_t^{t+\Delta t} \underline{i}'_c(\tau) d\tau$$

$$\underline{\lambda}(t+\Delta t) = \underline{\lambda}(t) + \int_t^{t+\Delta t} \underline{v}_L(\tau) d\tau$$

$$\underline{\lambda}'(t+\Delta t) = \underline{\lambda}(t) + \int_t^{t+\Delta t} \underline{v}'_L(\tau) d\tau$$

$$\underline{v}_c(t+\Delta t) = \underline{f}_S [\underline{q}(t+\Delta t), \underline{P}]$$

$$\underline{v}'_c(t+\Delta t) = \underline{f}_S [\underline{q}'(t+\Delta t), \underline{P}']$$

$$\underline{i}_L(t+\Delta t) = \underline{f}_I [\underline{\lambda}(t+\Delta t), \underline{P}]$$

$$\underline{i}'_L(t+\Delta t) = \underline{f}_I [\underline{\lambda}'(t+\Delta t), \underline{P}']$$

$$\underline{Y}(t+\Delta t) = \underline{F} \left[\begin{array}{l} \underline{v}_g(t+\Delta t), \underline{i}_g(t+\Delta t), \\ \underline{v}_c(t+\Delta t), \underline{i}_L(t+\Delta t), \underline{P} \end{array} \right]$$

$$\underline{Y}'(t+\Delta t) = \underline{F} \left[\begin{array}{l} \underline{v}_g(t+\Delta t), \underline{i}_g(t+\Delta t), \\ \underline{v}'_c(t+\Delta t), \underline{i}'_L(t+\Delta t), \underline{P}' \end{array} \right]$$

$$\Delta \underline{Y}(t+\Delta t) = \underline{Y}'(t+\Delta t) - \underline{Y}(t+\Delta t)$$

$$f[\mathbf{x}(t+\Delta t)] = f[\underline{v}_g(t+\Delta t), \underline{i}_g(t+\Delta t), \underline{v}_c(t+\Delta t), \underline{i}_L(t+\Delta t), P]$$

$$f'[\mathbf{x}(t+\Delta t)] = f[\underline{v}_g(t+\Delta t), \underline{i}_g(t+\Delta t), \underline{v}_c'(t+\Delta t), \underline{i}_L'(t+\Delta t), P']$$

$$\Delta f[\mathbf{x}(t+\Delta t)] = f'[\mathbf{x}(t+\Delta t)] - f[\mathbf{x}(t+\Delta t)]$$

$$S_f^{y_j}(t+\Delta t) = \frac{\Delta y_j(t+\Delta t)}{y_j(t+\Delta t)} \cdot \frac{f(t+\Delta t)}{\Delta f(t+\Delta t)}$$

The computations for $t+2\Delta t$ are performed by repeating the above equations.

The initial state is $(\underline{q}(t+\Delta t), \underline{\lambda}(t+\Delta t))$.

If single parameters of several functions vary, then the infinitesimal change of an output y_j ($\epsilon \underline{Y}$) is given by

$$dy_j = \frac{\partial y_j}{\partial P_1} dP_1 + \dots + \frac{\partial y_j}{\partial P_n} dP_n$$

where P_1, \dots, P_n represent the varying parameters for functions f_1, \dots, f_n .

A worst-case and its approximation can be expressed as

$$|dy_j| \leq \left[\left(\frac{\partial y_j}{\partial P_1} dP_1 \right)^2 + \dots + \left(\frac{\partial y_j}{\partial P_n} dP_n \right)^2 \right]^{1/2}$$

$$|\Delta y_j| \approx \left[\left(\frac{\partial y_j}{\partial P_1} \Delta P_1 \right)^2 + \dots + \left(\frac{\partial y_j}{\partial P_n} \Delta P_n \right)^2 \right]^{1/2}$$

$$\approx \left[(\Delta y_{1j})^2 + \dots + (\Delta y_{nj})^2 \right]^{1/2}$$

where Δy_{kj} is the variation in y_j if only parameter P_k varies.

The program will approximate the worst-case computation by repeating the sensitivity algorithm for each of the "n" functions having parameter variations.

As with sensitivity, Δy_{kj} is computed with regard to function variation. That is,

more than one parameter can vary in a function. Of course in each step of the "n" iterations, only one function will be considered to vary. The remaining will not change; i. e.,

$$f_1, f'_1, f_2, \dots, f_n \text{ used for } \Delta y_{2j}$$

$$f_1, f_2, f'_2, f_3, \dots, f_n \text{ used for } \Delta_{2j}$$

$$f_1, \dots, f_n, f'_n \text{ used for } \Delta y_{nj}$$

The outputs available in the worst case analysis will be $\underline{Y}(t)$ and $\Delta \underline{Y}(t)$ where $\underline{Y}(t)$ is computed for f_1, \dots, f_n and $\Delta \underline{Y}(t)$ is the approximate worst-case change.

APPENDIX F: COMPUTER MODELING OF NONLINEAR LINVILL PARAMETERS

The nonlinear analysis program, described in Section 4, has the potential for including nonlinear dependent sources which are functions of several variables. As an example β , for the dependent current source $i_c = \beta i_b$, can be a function of i_b and v_c . The equation $i_c = 10 i_b^2 (1 - e^{-Kv_c})$ is an illustration of a multivariable dependency. This manner of dependency can be applied to both dependent current sources and dependent voltage sources.

The property of multivariable dependency for controlled sources permits the modeling of nonlinear Linvill parameters. It develops that the behavior of each Linvill lump is affected by the junction. Furthermore, nonlinear interactions appear among the lumps. In the forthcoming development, it will be seen that these interactions can be represented by dependent current sources which are functions of several variables.

Four distinct analyses are required to discuss the manner of modeling.

These are:

- (1) The model of a Linvill lump which is between a junction (or depletion layer) and another lump.
- (2) The model of a Linvill lump which is straddled by two other lumps.
- (3) The model of a Linvill lump which is between a lump and the device terminal.
- (4) The model of the depletion layer. The four preceding models will be used to demonstrate a nonlinear Linvill diode representation. Also, the state equations of a simple circuit utilizing the diode will be determined.

The basic instantaneous Linvill equations required to model a lump which is between the junction and another lump are, following the development of Section 2:

$$i_1 = H_{d12}^n (n_1 - n_2) - H_{d12}^p (p_1 - p_2) + \frac{F_{d12}^n}{2} (n_1 + n_2) + \frac{F_{d12}^p}{2} (p_1 + p_2) \quad (F-1)$$

$$F_{d12}^n = \frac{q^2 \mu_n}{\epsilon} (n_1 - n_2) \quad (F-2)$$

$$(n_1 - n_2) = \frac{A\epsilon}{q \Delta x_{12}} (\Delta v_{12}) \quad (F-3)$$

$$F_{d12}^p = \frac{q^2 \mu_p}{\epsilon} (p_1 - p_2) \quad (F-4)$$

$$(p_1 - p_2) = \frac{A\epsilon}{q \Delta x_{12}} (\Delta v_{12}) \quad (F-5)$$

$$n_1 = n_0 e^{(q/kT) v_j} \quad (F-6)$$

$$p_1 = p_0 e^{(q/kT) v_j} \quad (F-7)$$

Since voltage and current rather than charge densities (n_1 , n_2 , p_1 , p_2) are the circuit variables of interest, a manipulation of equations (F-2) through (F-7) and a substitution into equation (F-1) will be made. This will avail a relationship in which the total lump current i_1 is a function of the junction voltage v_j and the lump voltage Δv_{12} .

Initially, equations (F-3) and (F-5) are substituted into equation (F-1).

The result is:

$$i_1 = H_{d12}^n \frac{A\epsilon}{q \Delta x_{12}} \Delta v_{12} - H_{d12}^p \frac{A\epsilon}{q \Delta x_{12}} \Delta v_{12} + \frac{F_{d12}^n}{2} (n_2 - n_1 + 2n_1) + \frac{F_{d12}^p}{2} (p_2 - p_1 + 2p_1) \quad (\text{F-8})$$

In the interest of simplicity, the following linear conductance is defined:

$$G_1 \triangleq (H_{d12}^n - H_{d12}^p) \frac{A\epsilon}{q \Delta x_{12}} \quad (\text{F-9})$$

By simultaneously substituting equations (F-3), (F-5), (F-6), (F-7), and (F-9) into (F-8); the following equation will result:

$$i_1 = G_1 \Delta v_{12} + \frac{F_{d12}^n}{2} \left[-\frac{A\epsilon}{q \Delta x_{12}} \Delta v_{12} + 2n_0 e^{(q/kT)v_j} \right] + \frac{F_{d12}^p}{2} \left[-\frac{A\epsilon}{q \Delta x_{12}} \Delta v_{12} + qp_0 e^{(q/kT)v_j} \right] \quad (\text{F-10})$$

The only quantities of equation (F-10) which directly relate to charge densities are F_{d12}^n and F_{d12}^p . By substituting (F-3) into (F-2) and (F-5) into (F-4), they can be made functions of the lump voltage.

$$F_{d12}^n = \frac{A\mu_n}{\Delta x_{12}} \Delta v_{12} \quad (\text{F-11})$$

$$F_{d12}^p = \frac{A\mu_p}{\Delta x_{12}} \Delta v_{12} \quad (\text{F-12})$$

Also in the interest of convenience, the following quantity is defined:

$$K \triangleq q/kT \quad (\text{F-13})$$

Substitution of (F-11) through (F-13) into (F-10) yields:

$$i_1 = G_1 (\Delta v_{12}) + \frac{A \mu_n}{2 \Delta x_{12}} \Delta v_{12} \left[-\frac{A \epsilon}{q \epsilon x_{12}} \Delta v_{12} + 2n_0 e^{Kv_j} \right] \\ + \frac{A \mu_p}{2 \Delta x_{12}} \Delta v_{12} \left[-\frac{A \epsilon}{q \Delta x_{12}} \Delta v_{12} + 2p_0 e^{Kv_j} \right] \quad (F-14)$$

Additional simplification is afforded by defining the following quantities:

$$A_1 \triangleq -\frac{A^2 \epsilon}{2q(\Delta x_{12})^2} (\mu_n + \mu_p) \quad (F-15)$$

$$B_1 \triangleq \frac{A}{\Delta x_{12}} (n_0 \mu_n + p_0 \mu_p) \quad (F-16)$$

The utilization of (F-15) and (F-16) allows (F-13) to be written as:

$$i_1 = G_1 \Delta v_{12} + A_1 (\Delta v_{12})^2 + B_1 \Delta v_{12} e^{Kv_j} \quad (F-17)$$

Equation (F-17) is the desired form. It indicates that the instantaneous part of the lump consists of three parallel elements. These are a linear conductance G_1 , a nonlinear conductance $A_1 \cdot (\Delta v_{12})$, and a nonlinear dependent current source $B_1 (\Delta v_{12}) e^{Kv_j}$. In addition to these three elements, the lump has a shunting capacitance which will be represented by C_1 .

The following equations will be used to determine the instantaneous model of a lump which is straddled by two other lumps. It will be assumed that one of the straddling lumps is adjacent to the depletion layer.

$$i_2 = H_{d23}^n (n_2 - n_3) - H_{d23}^p (p_2 - p_3) + \frac{F_{d23}^n}{2} (n_2 + n_3) + \frac{F_{d23}^p}{2} (p_2 + p_3) \quad (F-18)$$

$$F_{d23}^n = \frac{q^2 \mu_n}{\epsilon} (n_2 - n_3) \quad (F-19)$$

$$(n_2 - n_3) = \frac{A\epsilon}{q \Delta x_{23}} \Delta v_{23} \quad (\text{F-20})$$

$$F_{d23}^p = \frac{q \mu_p}{\epsilon} (p_2 - p_3) \quad (\text{F-21})$$

$$(p_2 - p_3) = \frac{A\epsilon}{q \Delta x_{23}} \Delta v_{23} \quad (\text{F-22})$$

The manipulations proceed in a manner similar to the preceding analysis.

A substitution of (F-20) and (F-22) into (F-18) yields:

$$\begin{aligned} i_2 = & H_{d23}^n \frac{A\epsilon}{q \Delta x_{23}} \Delta v_{23} - H_{d23}^n \frac{A\epsilon}{q \Delta x_{23}} \Delta v_{23} \\ & + \frac{F_{d23}^n}{2} \left[(n_3 - n_2) + 2(n_2 - n_1) + 2n_1 \right] \\ & + \frac{F_{d23}^p}{2} \left[(p_3 - p_2) + 2(p_2 - p_1) + 2p_1 \right] \end{aligned} \quad (\text{F-23})$$

The following conductance will now be defined:

$$G_2 \triangleq (H_{d23}^n - H_{d23}^p) \frac{A\epsilon}{q \Delta x_{23}} \quad (\text{F-24})$$

By substituting (F-3), (F-5), (F-6), (F-7), (F-20), (F-22), and (F-24) into

(F-23), the following results:

$$\begin{aligned} i_2 = & G_2 (\Delta v_{23}) + \frac{F_{d23}^n}{2} \left[- \frac{A\epsilon}{q \Delta x_{23}} \Delta v_{23} - \frac{2A\epsilon}{q \Delta x_{12}} \Delta v_{12} \right. \\ & \left. + 2n_0 e^{Kv_j} \right] + \frac{F_{d23}^p}{2} \left[- \frac{A\epsilon}{q \Delta x_{23}} \Delta v_{23} \right. \\ & \left. - \frac{2A\epsilon}{q \Delta x_{12}} \Delta v_{12} + 2p_0 e^{Kv_j} \right] \end{aligned} \quad (\text{F-25})$$

Observe that the current in the second lump from the junction depends upon the junction voltage v_j , the voltage across the first lump Δv_{12} , and its own voltage Δv_{23} . In general, the current of the N^{th} lump away from a junction will depend upon all N lump voltages. A recursive formulation can be determined for a general expression. This expression will not, however, be presented at this time.

One has from equations (F-19) through (F-22):

$$F_{d23}^n = \frac{A\mu_n}{\Delta x_{23}} \Delta v_{23} \quad (\text{F-26})$$

$$F_{d23}^p = \frac{A\mu_p}{\Delta x_{23}} \Delta v_{23} \quad (\text{F-27})$$

By substituting (F-26) and (F-27) into (F-25) and then substituting definitions (F-28) through (F-30), equation (F-31) will result.

$$A_2 \triangleq -\frac{A^2 \epsilon}{2q \Delta x_{23}} (\mu_n + \mu_p) \quad (\text{F-28})$$

$$B_2 \triangleq \frac{A}{\Delta x_{23}} (n_0 \mu_n + p_0 \mu_p) \quad (\text{F-29})$$

$$D_2 \triangleq -\frac{A^2 \epsilon}{q \Delta x_{12} \Delta x_{23}} (\mu_n + \mu_p) \quad (\text{F-30})$$

$$i_2 = G_2 \Delta v_{23} + A_2 (\Delta v_{23})^2 + B_2 \Delta v_{23} e^{Kv_j} + D_2 \Delta v_{12} \Delta v_{23} \quad (\text{F-31})$$

Equation (F-31) indicates that the instantaneous portion of the second lump consists of three parallel elements. They are: a linear conductance G_{12} , a

nonlinear conductance $A_2 \cdot (\Delta v_{23})$, and the nonlinear dependent current source $B_2 \Delta v_{23} e^{Kv_j} + D_2 \Delta v_{12} \Delta v_{23}$. The shunting lump capacitance will be designated by C_2 .

The third lump will be taken as the terminal part of the semiconductor.

The current for a terminal lump can be represented by:

$$\begin{aligned}
 i_3 &= qSA [(p_3 - p_0) - (n_3 - n_0)] \\
 i_3 &= qSA [(p_3 - p_0) - (n_3 - n_0)] \\
 &= qSA [(p_3 - p_2) + (p_2 - p_1) + (p_1 - p_0) + (n_0 - n_1) \\
 &\quad + (n_1 - n_2) + (n_2 - n_3)] \tag{F-32}
 \end{aligned}$$

The following equations will be substituted into (F-32), (F-3), (F-5), (F-6), (F-7), (F-20) and (F-22).

$$\begin{aligned}
 i_3 &= qSA \left[-\frac{A\epsilon}{q\Delta x_{23}} \Delta v_{23} - \frac{A\epsilon}{q\Delta x_{12}} \Delta v_{12} \right. \\
 &\quad \left. + p_0 (e^{Kv_j} - 1) + n_0 (1 - e^{Kv_j}) \right. \\
 &\quad \left. + \frac{A\epsilon}{q\Delta x_{12}} \Delta v_{12} + \frac{A\epsilon}{q\Delta x_{23}} \Delta v_{23} \right] \\
 &= qSA (p_0 - n_0) (e^{Kv_j} - 1) \tag{F-33}
 \end{aligned}$$

$$\text{Define: } A_3 \triangleq qSA (p_0 - n_0) \tag{F-34}$$

$$\text{Therefore: } i_3 = A_3 (e^{Kv_j} - 1) \tag{F-35}$$

Equation (F-35) indicates that the instantaneous portion of the terminal lump is a dependent current source. The lump capacitance will be designated by C_3 .

The depletion layer is representable by a nonlinear conductor shunted with a nonlinear capacitor. The relationships are given by:

$$f_{Gj}(v_j) = I_S e^{K(v_j + v_b)} - 1 \quad (F-36)$$

Where:

$$I_S = qA \left(p_0 \frac{D_p}{\tau_p} + n_0 \frac{D_n}{L_n} \right) \quad (F-37)$$

$$S_j = K_S (v_j + v_b)^{1/2} \quad (\text{elastance}) \quad (F-38)$$

Where:

$$K_S \triangleq \frac{1}{A} \frac{2(N_N + N_P)^{1/2}}{\epsilon q N_N N_P} \quad (F-39)$$

and N_N , N_P are the density of ionized impurity atom in the N- and P- regions respectively. The sign for the barrier voltage ($+v_b$) is for a positive current direction from "P" to "N" and the higher potential for v_j is in the "P" material.

In order to simulate nonlinear capacitors in the program, the capacitor voltage must be expressed as a function of charge. A simple manipulation of (F-38) provides this function.

$$v_j = f_{Sj}(q_j) = \frac{K_S}{2} \left(K_S q_j + (K_S q_j)^2 + 4v_b \right)^{1/2} q_j \quad (F-40)$$

Equation (F-40) applies for the region in which $v_j > -v_b$.

The circuit shown in Figure F1 will be used to illustrate an application of the preceding development.

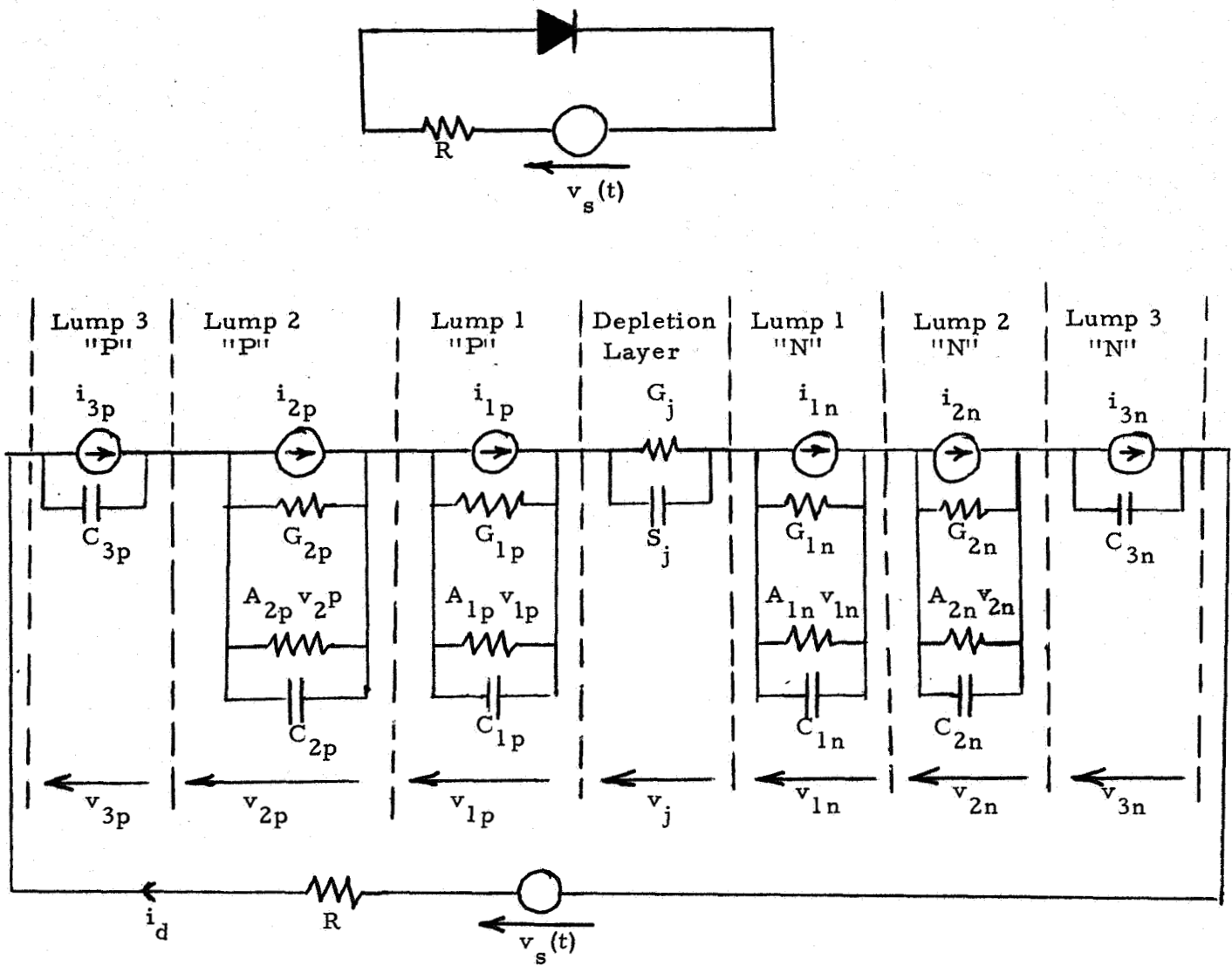


Figure F1. Equivalent Diode Circuit

The relationships for the dependent sources are given in the following. Note that the subscript "y" assumes both "n" and "p" in the circuit.

$$i_{1y} = B_{1y} v_{1y} e^{Kv_j} \quad (F-41)$$

$$i_{2y} = (B_{2y} e^{Kv_j} + D_{2y} v_{1y}) v_{2y} \quad (F-42)$$

$$i_{3y} = A_{3y} (e^{Kv_j} - 1) \quad (F-43)$$

The diode voltage and the diode current can be determined from equations (F-44) and (F-45).

$$v_d = v_{3p} + v_{2p} + v_{1p} + v_j + v_{1n} + v_{2n} + v_{3n} \quad (F-44)$$

$$i_d = \frac{1}{R_s} (v_s - v_d) \quad (F-45)$$

The equations for the seven capacitor currents are tantamount to the state equations. The currents need to be functions of the seven capacitor voltages and the independent source v_s . For convenience, the equations and the independent source v_s . For convenience, the equations will be written in terms of relationships (F-41) through (F-45). Again "y" represents "n" and "p".

$$i_{c3y} = i_d - i_{3y} \quad (F-46)$$

$$i_{c2y} = i_d - i_{2y} - G_{2y} v_{2y} - A_{2y} v_{1y}^2 \quad (F-47)$$

$$i_{c1y} = i_d - i_{1y} - G_{1y} v_{1y} - A_{1y} v_{1y}^2 \quad (F-48)$$

$$i_{sj} = i_d - G_j v_j = i_d - I_S [e^{K(v_j + v_b)} - 1] \quad (F-49)$$

Environmental effects, such as radiation and temperature, may be represented through the Linvill parameters, as before, and Eqs. (F-13) and (F-37). Nonlinear transistor analysis may be performed in a manner similar to the diode analysis described above.